

Efficient Transformed Gaussian Processes for Non-Stationary Dependent Multi-class Classification

Juan Maroñas
Machine Learning Group
Universidad Autónoma de Madrid
Madrid, Spain
juan.maronnas@uam.es

Daniel Hernández-Lobato
Machine Learning Group
Universidad Autónoma de Madrid
Madrid, Spain
daniel.hernandez@uam.es

Abstract

This work introduces the Efficient Transformed Gaussian Process (ETGP), a new way of creating C stochastic processes characterized by: 1) the C processes are *non-stationary*, 2) the C processes are dependent by construction without needing a mixing matrix, 3) training and making predictions is very efficient since the number of Gaussian Processes (GP) operations (e.g. inverting the inducing point’s covariance matrix) do not depend on the number of processes. This makes the ETGP particularly suited for multi-class problems with a very large number of classes, which are the problems studied in this work. ETGPs exploit the recently proposed Transformed Gaussian Process (TGP), a stochastic process specified by transforming a Gaussian Process using an invertible transformation. However, unlike TGPs, ETGPs are constructed by transforming a single sample from a GP using C invertible transformations. We derive an efficient sparse variational inference algorithm for the proposed model and demonstrate its utility in 5 classification tasks which include low/medium/large datasets and a different number of classes, ranging from just a few to hundreds. Our results show that ETGPs, in general, outperform state-of-the-art methods for multi-class classification based on GPs, and have a lower computational cost (around one order of magnitude smaller).

1 Introduction

Gaussian Processes (GPs) are stochastic processes characterized by their finite-dimensional distributions being multivariate Gaussian [32], and have become a uniquely popular modeling tool. For example, in the machine learning community GPs are used as prior distributions over functions, used to solve tasks such as regression, classification, feature extraction or hyper-parameter optimization [32, 24, 39]. Their non-parametric nature imply that they become more expressive with more data [32]. Furthermore, GPs are characterized by a predictive distribution which provides information about what the model does not know [14] and are easy to interpret since the covariance function gives insights about the nature of the latent function to be inferred [13]. GPs have also been applied in spatial statistics [23], and to explain physics phenomena such as those that arise when studying molecular dynamics [26, 44]. Moreover, they are used as a theoretical tool to understand Deep Neural Networks (DNN) [30, 51] and lie at the core of a recent family of Deep Generative Models that generate samples attending to the dynamics of a diffusion process [41].

Here, we focus on multi-class classification problems with $C > 2$ classes. For this, one often defines C independent GPs, one per each class [32]. In this case, the number of GP operations (such as inverting the kernel matrix over the inducing points) grows linearly with C . Thus, if C is large, this can be too expensive. Some speed-up tricks include sharing the inducing points or the kernel across each GP but often reduce the performance of the classifier, as we show in our experiments. Even with this trick, computing the parameters of the predictive distribution still has complexity $\mathcal{O}(CM^2)$ per datapoint. We can gain additional performance by defining a prior using C dependent GPs, which can be done by mixing Q latent GPs with a mixing matrix $\Phi \in \mathbb{R}^{Q \times C}$. However, in practice, these dependencies are often ignored since the memory complexity scales as $\mathcal{O}(C^2)$ per datapoint. In fact,

modern SOTA GP software’s like GPFLOW [29, 45] require significant source code modification (up to early 2022) to handle these dependencies in an efficient way.

A disadvantage of GPs is that they usually impose strong assumptions about the nature of the latent function. For example, most covariance functions are stationary and assume a constant level of smoothness for the latent function on the input domain [32]. If this is not the case, the performance can be degraded. However, GPs can be made more expressive using non-stationary processes, but this is usually only justified if one has background knowledge about the nonstationarity of the particular application. For example, for Bayesian Optimization [40], Geostatistics [46, 50, 18, 35, 36] or temporal gene expression [19].

The flexibility of GPs can also be increased by non-linearly transforming these processes. Examples include deep GPs (DGPs) [12] and transformed GPs (TGPs) [28]. In DGPs, the output of a GP is used as the input of another GP systematically, following a fully connected neural network (NN) architecture in which units are GPs. As a result of the concatenation, the resulting process need not be stationary. In TGPs the initial GP prior is transformed iteratively using input-dependent invertible transformations [28]. Because of this input dependence, the resulting process need not be stationary. Importantly, TGPs often generate models that are as accurate as DGPs at a lower computational cost.

In this work we introduce the Efficient Transformed Gaussian Process (ETGP), a new model where C processes are specified by sampling from a single GP, and then transforming this sample using C invertible transformations (throughout the paper we refer to the invertible transformations by flows or warping functions as well). By this construction, the C processes are non-stationary and dependent, with dependencies modeled by the copula of the base GP and without the computational and memory complexity of an equivalent number of GPs, since only one GP is used in the construction of the C processes. A special case of the ETGP family specified by using a linear flow includes non-stationary dependent GPs, which we also characterize and study. We evaluate the prediction performance and computational cost of ETGP in the context of multi-class problems with a large number of classes C . With this goal, we derive an efficient sparse variational inference (VI) algorithm for ETGP. We carry out experiments across several classification tasks which include small and large datasets and up to 153 class labels. The results obtained show that ETGPs, in general, outperform SOTA methods for multi-class classification based on GPs, and that they have a computational cost that is around one order of magnitude smaller. Our experiments also show that non-stationary covariances are not useful for black-box function approximations and that the particular inductive bias of the ETGP is rather much more beneficial.

2 Background

We start by introducing GPs for multi-class classification problems and some notation. We also describe how to improve GPs using the TGP method.

2.1 Multi-class Gaussian process classification

Consider the problem of assigning a class label $y \in \mathcal{Y} = \{1, \dots, C\}$, with C the number of classes, to an input $\mathbf{x} \in \mathcal{X} \subseteq \mathbb{R}^d$. Our goal is to learn a set of C functions mapping \mathbf{x} to class label probabilities. For this, we are given a set of N labeled instances $\mathcal{D} = \{\mathbf{x}^n, y^n\}_{n=1}^N$ generated from the data distribution, and define $\mathbf{X} = (\mathbf{x}^1, \dots, \mathbf{x}^N)$ and $\mathbf{y} = (y^1, \dots, y^N)$. We model these functions in a Bayesian way by placing an independent GP over each of them, which is updated into a posterior over functions given \mathcal{D} , used to obtain a predictive distribution for the label associated to new data.

A GP is a stochastic process whose finite-dimensional distributions are given by a multivariate Gaussian. Specifically, let $\mathbf{f} = (f(\mathbf{x}^1), \dots, f(\mathbf{x}^N))^T$ and define $f_n := f(\mathbf{x}^n)$. Then, $\mathbf{f} \sim \mathcal{N}(\mu_\nu(\mathbf{X}), K_\nu(\mathbf{X}, \mathbf{X}))$, where the mean vector $\mu_\nu(\mathbf{X}) = (\mu_\nu(\mathbf{x}^1), \dots, \mu_\nu(\mathbf{x}^N))^T$ is obtained by a mean function $\mu_\nu : \mathcal{X} \rightarrow \mathbb{R}$, and $K_\nu(\mathbf{x}, \mathbf{x})$ is a $N \times N$ matrix whose i -th row and j -th column are given by $K_\nu(\mathbf{x}^i, \mathbf{x}^j)$, obtained by a covariance function $K_\nu : \mathcal{X} \times \mathcal{X} \rightarrow \mathbb{R}$; both parameterized by ν . Without loss of generality, in the rest of the paper we assume zero mean GPs.

Consider C independent GPs and denote $\bar{\mathbf{f}} = \{\mathbf{f}^1, \dots, \mathbf{f}^C\}$, where a bar over a letter \bar{x} summarizes the corresponding C elements x^1, \dots, x^C . Often, a Softmax link function $\pi_c(\bar{f}_n) = \exp(f^c(\mathbf{x}^n)) / \sum_{c'=1}^C \exp(f^{c'}(\mathbf{x}^n))$ is applied to $\bar{\mathbf{f}}$ to turn them into class label probabilities π_c [32].

Then, these probabilities are linked to actual class labels \mathbf{y} by a categorical likelihood. Under these conditions, the joint distribution of \mathbf{y} and $\bar{\mathbf{f}}$ is:

$$p(\mathbf{y}, \bar{\mathbf{f}}) = p(\mathbf{y} | \bar{\mathbf{f}})p(\bar{\mathbf{f}}) = \left[\prod_{n=1}^N \prod_{c=1}^C \pi_c(\bar{f}_n)^{\mathbb{I}(y^n=c)} \right] \prod_{c=1}^C \mathcal{N}(\mathbf{f}^c | \mathbf{0}, K_\nu^c(\mathbf{X}, \mathbf{X})), \quad (1)$$

where \mathbb{I} represents the indicator function. To make predictions we need to approximate the intractable posterior $p(\bar{\mathbf{f}} | \mathcal{D})$. We rely on the sparse variational inference (VI) approximation [10, 43] with the modifications introduced in [21] to scale to very large datasets.

Sparse variational GPs (SVGPs) work by introducing a set of $M \ll N$ inducing points locations $\mathbf{Z} = (\mathbf{z}^1, \dots, \mathbf{z}^M)$, $\mathbf{z} \in \mathcal{X}$ with associated GP outputs $\mathbf{u} = (f(\mathbf{z}^1), \dots, f(\mathbf{z}^M))^T$ per each of the C functions, with joint Gaussian prior $p(\bar{\mathbf{f}}, \bar{\mathbf{u}} | \mathbf{X}, \bar{\mathbf{Z}})$ obtained with the prior covariance function. These inducing points act as sufficient statistics of the data \mathbf{x} , with the purpose of representing the posterior $p(\bar{\mathbf{f}} | \mathcal{D})$ using M points, reducing the complexity from $\mathcal{O}(CN^3)$ [32] to $\mathcal{O}(CM^3)$ [43]. The key point in [43] is to treat $\bar{\mathbf{Z}}$ as variational parameters, which are optimized by minimizing the Kullback-Leibler Divergence (KLD) between a variational posterior $q(\bar{\mathbf{f}}, \bar{\mathbf{u}})$ and the augmented joint posterior $p(\bar{\mathbf{f}}, \bar{\mathbf{u}} | \mathcal{D}, \bar{\mathbf{Z}})$, or equivalently by maximizing the Evidence Lower Bound (ELBO). Since $\bar{\mathbf{Z}}$ are variational parameters, they are protected from overfitting. The speed-up is achieved by constraining the form of the variational distribution $q(\bar{\mathbf{f}}, \bar{\mathbf{u}}) = \prod_{c=1}^C p(\mathbf{f}^c | \mathbf{u}^c)q(\mathbf{u}^c)$, which is defined using the conditional model's prior $p(\mathbf{f}^c | \mathbf{u}^c)$ and a Gaussian variational distribution $q(\mathbf{u}^c)$ with mean and covariance matrix $\mathbf{m}^c \in \mathbb{R}^M$ and $\mathbf{S}^c \in \mathbb{R}^{M \times M}$. With this, the ELBO is:

$$\text{ELBO} = \sum_{n=1}^N \sum_{c=1}^C \mathbb{I}(y^n=c) \mathbb{E}_q [\log \pi_c(\bar{f}_n)] - \sum_{c=1}^C \text{KLD}[q(\mathbf{u}^c) || p(\mathbf{u}^c)], \quad (2)$$

where $\text{KLD}[q(\mathbf{u}^c) || p(\mathbf{u}^c)]$ can be computed in closed form and the expectation with respect to q can be approximated by Monte Carlo. The above expression allows to use stochastic VI to optimize the ELBO [21], by sub-sampling the data using mini-batches [21]. We use path-wise derivatives for black-box low-variance gradient estimations. The variational distribution $q(f^c(\mathbf{x}^n) | \mathbf{u}^c)q(\mathbf{u}^c)d\mathbf{u}^c$ is Gaussian with mean and covariance given by $K_\nu^c(\mathbf{x}^n, \mathbf{Z}^c)K_\nu^c(\mathbf{Z}^c, \mathbf{Z}^c)^{-1}\mathbf{m}^c$ and $K_\nu^c(\mathbf{x}^n, \mathbf{x}^n) - K_\nu^c(\mathbf{x}^n, \mathbf{Z}^c)K_\nu^c(\mathbf{Z}^c, \mathbf{Z}^c)^{-1}[K_\nu^c(\mathbf{Z}^c, \mathbf{Z}^c) + \mathbf{S}^c]K_\nu^c(\mathbf{Z}^c, \mathbf{Z}^c)^{-1}K_\nu^c(\mathbf{Z}^c, \mathbf{x}^n)$, respectively. The predictive distribution for the label y^* associated to a new point \mathbf{x}^* , can also be approximated via Monte Carlo by sampling from $q(f^c(\mathbf{x}^*))$ for $c = 1, \dots, C$.

2.2 Transformed Gaussian Processes

A limitation of GPs is that they place strong assumptions over the latent function. This can be for example assuming the same level of smoothness across the input domain, as it is often done by considering a stationary covariance function [32]. The Transformed Gaussian Process (TGP) [28] is a model that increases the flexibility of GPs by non-linearly and input-dependently transforming the GP prior using invertible transformations. We describe the TGP, since is the building block of the proposed approach.

Let $f_0(\cdot) \sim \text{GP}(0, K_\nu(\cdot, \cdot))$ be a sample from a GP. Consider a composition of individual invertible functional mappings $\mathbb{G}_{\theta_K} = \mathbb{G}_{\theta_0} \circ \mathbb{G}_{\theta_1} \dots \circ \mathbb{G}_{\theta_{K-1}} : \mathcal{F}_0 \rightarrow \mathcal{F}_K$ each parameterized by $\theta \in \Theta$. The TGP, is defined by the following generative procedure:

$$f_0(\cdot) \sim \text{GP}(0, K_\nu(\cdot, \cdot)), \quad f_K(\cdot) = \mathbb{G}_{\theta_K}(f_0(\cdot)). \quad (3)$$

An easy way to specify \mathbb{G}_{θ_K} so that f_K is a consistent process (i.e. a process satisfying the Kolmogorov extension theorem) is to use element-wise mappings (also known by diagonal flows), characterized by: $\forall \mathbf{x}^n \in \mathcal{X}, f_K(\mathbf{x}^n) = \mathbb{G}_{\theta_K}(f_0(\mathbf{x}^n))$, as described in [33]¹. Due to these element-wise mappings, the resulting process is a Gaussian Copula process [48] since it has arbitrary marginals with dependencies driven by the copula of the GP, something derived from Sklar's theorem [37]. In other words, f_0 and f_K share the same dependencies but differ in their marginal distributions. By increasing K , we can make the flow as complicated as we want, increasing flexibility.

The work in [28] shows how to create non-stationary processes f_K by making the parameters of the flow depend on the input using a Neural Network (NN) $\text{NN} : \mathcal{X} \rightarrow \Theta$ parameterized by \mathbf{W} . In [28] they show that this non-stationary process is way more expressive than a GP and also than a stationary

¹The presented method and inference algorithm, and all the equations involved, assumes diagonal flows. One needs to check particularities that might arise for non-diagonal ones, see e.g. the appendix of [28]. Furthermore, any additional details about the equations in this paper and their derivation are given in App. A.

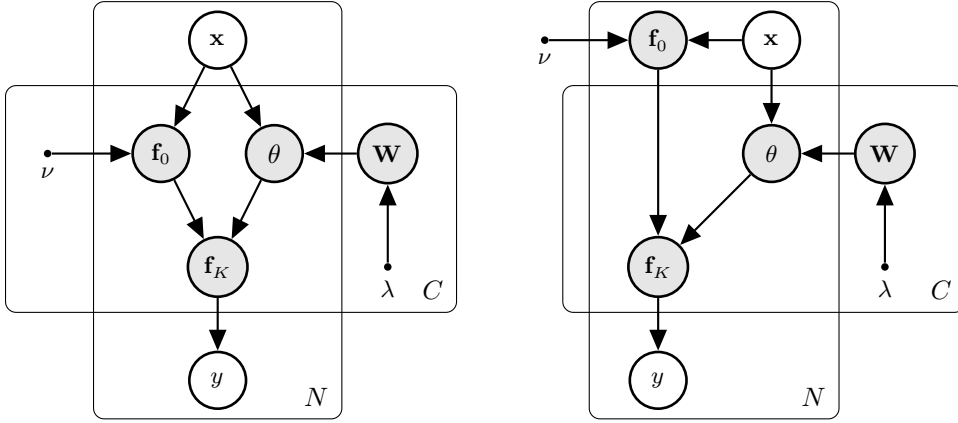


Figure 1: Probabilistic Graphical models for the TGP (left) and the ETGP (right).

TGP. Since the parameters of the NN play the same role of hyper-parameters in a GP, this work shows how using a Bayesian Neural Network (BNN) can effectively avoid over-fitting as this makes the NN’s parameters play the same role in the graphical model as GP’s latent functions, see Fig. 1.

For a classification problem, we can write the joint conditional distribution over the C independent TGPs by applying the change of variable formula and inverse function theorem [28]:

$$p(\bar{\mathbf{f}}_K | \bar{\mathbf{W}}) = \prod_{c=1}^C p(\mathbf{f}_0 | \nu^c) \prod_{k=0}^{K^c-1} \left| \det \frac{\partial \mathbb{G}_{\theta_k^c(\mathbf{w}^c, \mathbf{x})}(\mathbf{f}_k^c)}{\partial \mathbf{f}_k^c} \right|^{-1}. \quad (4)$$

This warping procedure can also be used when defining a variational approximation $q(\mathbf{f}_K, \mathbf{u}_K) = p(\mathbf{f}_K | \mathbf{u}_K)q(\mathbf{u}_K)$, where the cancellations of several factors in the ELBO result in an efficient training algorithm, as described in [28].

3 Efficient Transformed Gaussian Processes

In this section we describe the proposed method for multi-class GP classification, which we show is a more efficient application of the TGP to classification problems with large C ; with the additional benefit of naturally modeling dependencies between the processes. Our proposed method is specified by transforming a single sample from a GP using C invertible transformations, each of them mapping the GP to a latent function for each class label. The generative procedure is given by:

$$f_0(\cdot) \sim \text{GP}(0, K_\nu(\cdot, \cdot)), \quad f_K^1(\cdot) = \mathbb{G}_{\theta_K^1(\mathbf{w}^1, \mathbf{x})}^1(f_0(\cdot)), \quad \dots \quad f_K^C(\cdot) = \mathbb{G}_{\theta_K^C(\mathbf{w}^C, \mathbf{x})}^C(f_0(\cdot)). \quad (5)$$

Using again the change of variable formula and inverse function theorem employed in Sec. 2.2, the joint conditional distribution of the C processes is given by:

$$p(\bar{\mathbf{f}}_K | \bar{\mathbf{W}}) = p(\mathbf{f}_0) \prod_{k=0}^{K^1-1} \left| \det \frac{\partial \mathbb{G}_{\theta_k^1(\mathbf{w}^1, \mathbf{x})}(\mathbf{f}_k^1)}{\partial \mathbf{f}_k^1} \right|^{-1} \prod_{c=2}^C \delta(\mathbf{f}_K^c - \mathbb{G}_{\theta_K^c(\mathbf{w}^c, \mathbf{x})}^c \circ \mathbb{H}_{\theta_K^1(\mathbf{w}^1, \mathbf{x})}^1(\mathbf{f}_K^1)), \quad (6)$$

where $\delta(\cdot)$ denotes the Dirac measure and we define $\mathbb{H} = \mathbb{G}^{-1}$ to be the corresponding inverse transformation. Note that this decomposition is not unique. We label \mathbf{f}_K^1 as the *pivot* and note that this joint distribution can be written equivalently w.r.t. any other *pivot* \mathbf{f}_K^c with $c \neq 1$.

This formulation has the advantage that a single GP is used in practice which implies a constant scaling of GP operations w.r.t. the number of classes, speeding-up computations. This contrasts with a naive use of TGPs or the model described in Sec. 2.1 and motivates the name given to our model which we call *Efficient Transformed Gaussian Processes* (ETGP), particularly suited for multi-class problems with large C . Moreover, the resulting C processes are dependent since they share the same latent sample f_0 from the original process. Also, since we use NNs to parameterize the flows, the C processes are non-stationary. Fig. 1 compares the graphical models of the naive use of TGP for multi-class classification and the proposed method ETGP, highlighting their differences.

Since our work is focused on presenting ETGPs as a good performance method at a low computational cost, we also propose an efficient NN parameterization of the flow parameters, illustrated in Fig. 2. In principle, we could use a NN per flow parameter, implemented efficiently using batched operations [6]. However, by using a single NN whose output layer coincides with the number of parameters per flow times the number of classes, we achieve a more efficient parameterization. For example, if we are modeling Imagenet ($C = 1000$) with a linear flow ($|\theta| = 2$), then we would use an output layer of 2000 neurons. Beyond being more efficient, this could also serve as a possible regularizer in the same fashion as sharing parameters regularizes DNNs, something commonly used in computer vision applications through a back-bone convolutional model.

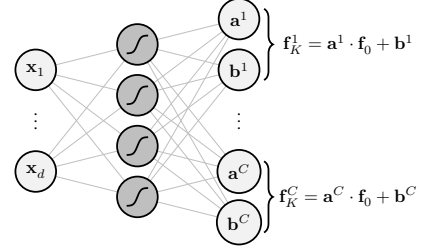


Figure 2: Architecture of the NN used in this work. Hidden layers are shared, with the final layer giving each of the parameters of the C flows.

Another appealing property of the ETGP is that we can efficiently create C non-stationary dependent GPs, by using a linear flow: $f_K(\mathbf{x}) = a(\mathbf{x})f_0(\mathbf{x}) + b(\mathbf{x})$, as shown in Fig. 2. The following proposition characterizes the corresponding joint prior distribution $p(\bar{\mathbf{f}}_K)$:

Proposition 1. *The joint conditional distribution of C non-stationary GPs obtained via a linear flow is given by:*

$$p(\bar{\mathbf{f}}_K | \bar{\mathbf{W}}) = \mathcal{N}(\mathbf{f}_K^1 | \mathbf{b}^1, \mathbf{A}_1 K_\nu(\mathbf{X}, \mathbf{X}) \mathbf{A}_1^T) \prod_{c=2}^C \delta(\mathbf{f}_K^c - \mathbb{G}_{\theta_K^c}^c(\mathbf{W}^c, \mathbf{X}) \circ \mathbb{H}_{\theta_K^c}^1(\mathbf{w}^1, \mathbf{X})(\mathbf{f}_K^1)), \quad (7)$$

with $\mathbf{b}^1 = (b^1(\mathbf{x}^1), \dots, b^1(\mathbf{x}^N))^T$ and $\mathbf{A}_1 \in \mathbb{R}^{N \times N}$ a diagonal matrix with entries $\mathbf{a}^1 = (a^1(\mathbf{x}^1), \dots, a^1(\mathbf{x}^N))^T$. Each marginal $p(\mathbf{f}_K^c)$ is Gaussian with mean and covariance given by \mathbf{b}^c and $\mathbf{A}_c K_\nu(\mathbf{X}, \mathbf{X}) \mathbf{A}_c^T$, respectively. The covariance matrix between the pivot \mathbf{f}_K^1 and \mathbf{f}_K^c , for $c \neq 1$, is given by: $\mathbf{a}^1 (\mathbf{a}^c)^T \odot K_\nu(\mathbf{X}, \mathbf{X})$ with \odot denoting Hadamard product. Proof given in App. A.

3.1 Approximate Inference

Our inference algorithm is inspired by the key observations of [43, 21, 28]. More precisely, we rely on a sparse VI algorithm where the variational distribution is defined so that the conditional's model prior $p(\mathbf{f}_K | \mathbf{u}_K)$ cancels [43], without marginalizing out the process values at the inducing points to allow for mini-batch optimization SVI [21], and by defining the variational distribution over the GP space and then warping it with the same flows as the prior [28].

To start with, a set of M inducing points is defined on the GP space $f_0(\cdot)$. Note, however, that we can easily extend our framework to use inter domain inducing points [25] since we just need to derive the corresponding cross-covariances. Let $\bar{\mathbf{u}}_K$ be defined as $\bar{\mathbf{f}}_K$ in Eq. 6 summarizing the C transformed process values at the inducing points \mathbf{Z} . In App. A we show that the joint conditional prior is:

$$p(\bar{\mathbf{f}}_K, \bar{\mathbf{u}}_K | \bar{\mathbf{W}}) = p(\mathbf{f}_0 | \mathbf{u}_0) \prod_{k=0}^{K^1-1} \left| \det \frac{\partial \mathbb{G}_{\theta_K^1}^1(\mathbf{w}^1, \mathbf{X})(\mathbf{f}_k^1)}{\partial \mathbf{u}_k^1} \right|^{-1} \prod_{c=2}^C \delta(\mathbf{f}_K^c - \mathbb{G}_{\theta_K^c}^c(\mathbf{W}^c, \mathbf{X}) \circ \mathbb{H}_{\theta_K^c}^1(\mathbf{w}^1, \mathbf{X})(\mathbf{f}_K^1)) \\ p(\mathbf{u}_0) \prod_{k=0}^{K^1-1} \left| \det \frac{\partial \mathbb{G}_{\theta_K^1}^1(\mathbf{w}^1, \mathbf{Z})(\mathbf{u}_k^1)}{\partial \mathbf{u}_k^1} \right|^{-1} \prod_{c=2}^C \delta(\mathbf{u}_K^c - \mathbb{G}_{\theta_K^c}^c(\mathbf{W}^c, \mathbf{Z}) \circ \mathbb{H}_{\theta_K^c}^1(\mathbf{w}^1, \mathbf{Z})(\mathbf{u}_K^1)) \quad (8)$$

This is possible because ETGP is a consistent process, which means we can extend its finite dimensional distribution with inducing point locations as in standard GPs. See [28] for further details.

The variational distribution is assumed to have a similar form to the prior with some factors that are shared between them and others that are specific of the posterior approximation: $q(\bar{\mathbf{f}}_K, \bar{\mathbf{u}}_K, \bar{\mathbf{W}}) = q(\bar{\mathbf{f}}_K, \bar{\mathbf{u}}_K | \bar{\mathbf{W}}) q(\bar{\mathbf{W}})$ as in [28], where the variational distribution over the NN has parameters $\bar{\phi}$ and is assumed to factorize across classes. Following [43, 28], the variational distribution over the values of the random processes at \mathbf{X} and \mathbf{Z} , $q(\bar{\mathbf{f}}_K, \bar{\mathbf{u}}_K) = p(\bar{\mathbf{f}}_K | \bar{\mathbf{u}}_K) q(\bar{\mathbf{u}}_K)$, is defined using the conditionals model's prior $p(\bar{\mathbf{f}}_K | \bar{\mathbf{u}}_K)$, given in Eq. 8, and a free form variational distribution $q(\bar{\mathbf{u}}_K)$. As in [28], $q(\bar{\mathbf{u}}_K)$ is defined by warping a multivariate Gaussian defined on the original f_0 space $q(\mathbf{u}_0 | \mathbf{m}, \mathbf{S})$ using \mathbb{G} , where $\mathbf{m} \in \mathbb{R}^M$, $\mathbf{S} \in \mathbb{R}^{M \times M}$ are the mean and covariance variational parameters:

$$q(\bar{\mathbf{u}}_K) = q(\mathbf{u}_0) \prod_{k=0}^{K^1-1} \left| \det \frac{\partial \mathbb{G}_{\theta_K^1}^1(\mathbf{w}^1, \mathbf{Z})(\mathbf{u}_k^1)}{\partial \mathbf{u}_k^1} \right|^{-1} \prod_{c=2}^C \delta(\mathbf{u}_K^c - \mathbb{G}_{\theta_K^c}^c(\mathbf{W}^c, \mathbf{Z}) \circ \mathbb{H}_{\theta_K^c}^1(\mathbf{w}^1, \mathbf{Z})(\mathbf{u}_K^1)) \quad (9)$$

The resulting ELBO on the log-marginal-likelihood is, after several factor cancellations, equal to:

$$\begin{aligned} \text{ELBO} = & \sum_{n=1}^N \sum_{c=1}^C \mathbb{I}(y^n = c) \mathbb{E}_{q(f_{0,n})q(\overline{\mathbf{W}})} [\log \pi_c(\mathbb{G}_{\theta_K}^1(\mathbf{W}^1, \mathbf{x}^n)(f_{0,n}), \dots, \mathbb{G}_{\theta_K}^C(\mathbf{W}^C, \mathbf{x}^n)(f_{0,n}))] \\ & - \text{KLD}[q(\mathbf{u}_0)||p(\mathbf{u}_0)] - \sum_{c=1}^C \text{KLD}[q(\mathbf{W}^c)||p(\mathbf{W}^c)] \end{aligned} \quad (10)$$

where $q(f_0)$ is computed as in Sec. 2.1. The expectation w.r.t. $q(\overline{\mathbf{W}})$ is computed via Monte Carlo and a single 1-d quadrature is used to compute expectations over $q(f_0)$. $\text{KLD}[q(\mathbf{u}_0)||p(\mathbf{u}_0)]$ is tractable. $\text{KLD}[q(\mathbf{W}^c)||p(\mathbf{W}^c)]$ can be computed in closed-form for certain choices of the prior and variational posterior. However, we follow [28] and use Monte Carlo Dropout [15] (MCDROP) rather than VI to perform inference on \mathbf{W} . With this, the same NN can be used to make non-Bayesian point estimate predictions (PE-ETGP) [42] or Bayesian predictions (BA-ETGP) [15]. This objective can be maximized using stochastic optimization methods and the data can be sub-sampled for mini-batch training. Readers concerned with the cancellation of delta functions in Eq. 10 can replace them with Gaussians with variance σ^2 to then take the limit $\sigma^2 \rightarrow 0$.

Predictions for y^* associated to a new \mathbf{x}^* are computed using an approximate predictive distribution:

$$p(y^* | \mathbf{x}^*, \mathcal{D}) \approx \mathbb{E}_{q(f_0(\mathbf{x}^*))q(\overline{\mathbf{W}})} [p(y^* | \mathbb{G}_{\theta_K}^1(\mathbf{W}^1, \mathbf{x}^*)(f_0(\mathbf{x}^*)), \dots, \mathbb{G}_{\theta_K}^C(\mathbf{W}^C, \mathbf{x}^*)(f_0(\mathbf{x}^*)))], \quad (11)$$

where the integral is approximated by Monte Carlo and 1-d quadrature having marginalized out $\overline{\mathbf{u}}_K$.

3.2 Summary of the proposed method and computational cost

ETGP creates C dependent processes since \mathbf{f}_0 is shared. We have characterized the dependencies of these C processes for a linear flow in Prop. 1. The flows, however, need not be linear and can be arbitrarily complicated. Because $\mathbb{G}_{\theta_K}^c$ is input-dependent the C processes are also non-stationary.

Expectations w.r.t. the NN’s parameters can be computed using batched matrix multiplications. Expectations w.r.t. $q(\mathbf{f}_0)$ in Eq. 10 and Eq. 11 can be computed with 1-d quadrature. By contrast, the SVGP method from Sec. 2.1 cannot use quadrature methods. Moreover, the number of GP operations is constant with C . To get $q(\mathbf{f}^c)$ in SVGPs Sec. 2.1 one needs a cubic operation to invert $K_\nu^c(\mathbf{z}, \mathbf{z})$ and M^2 operation to compute the variational parameters per class and datapoint, giving a complexity of $\mathcal{O}(CM^3 + CNM^2)$. This can be alleviated by sharing K_ν and \mathbf{Z} across GPs, resulting in $\mathcal{O}(M^3 + CNM^2)$, at the cost of limiting expressiveness, as we’ll show. ETGP cost is always $\mathcal{O}(M^3 + NM^2)$ (without considering the NN’s computations, which for the architecture presented is often much faster and can be done in parallel to GP operations).

4 Related Work

On the non-stationary side, the traditional approach is to use non-stationary covariance functions such as the Neural Network [47] or the Arcosine [11]. Our experiments, however, show that ETGP provides superior results in the multi-class setting when compared to a method using these kernels. One can also make stationary kernels non-stationary by making the parameters of the kernel depend on the input [19]. However, the work in [19] is limited to small datasets since it does not consider sparse GPs and it relies on Hamilton Monte Carlo for approximate inference, which is computationally expensive. Nevertheless, a sparse approach would require a GP per kernel hyperparameter which can lead to a big number of GPs for high d . Another approach to obtain non-stationary processes considers stochastic processes mixing using hierarchical models [46] or by placing GPs over the mixing matrix entries, achieving input-dependent length scales and amplitudes [50]. These works either don’t scale for high C [50] or require domain knowledge to avoid misspecification [46].

Non-stationarity can also be obtained by warping the input space using a non-linear transformation before introducing the data into the kernel [35, 36, 9, 49]. These methods, however, either run the risk of over-fitting the observed data, as a consequence of not regularizing the parameters of the non-linear transformation nor using a fully Bayesian approach, or either do not scale to large datasets.

One can also use more sophisticated processes such as the GP Product Model [2], DGPs [12] or TGPs [28] to achieve non-stationarity. The GP Product Model, however, does not scale to large datasets. DGPs have been shown to give similar results to those of TGPs. However, TGPs have a

lower computational cost than DGPs and slightly higher than SVGPs. Therefore, the proposed method, ETGP, is expected to be faster than TGPs and also faster than DGPs, in consequence.

On the dependence point of view, several approaches have been considered, which range from using process convolutions [7] to mix latent GPs via a mixing matrix [4] whose entries can be parameterized by a GP [50]. More recently, [22] extends Multi-output GPs [4], Gaussian Process Regression Networks [50] and DGP [12] by using NNs to replace different building blocks of these methods. Since the computational cost of considering several GPs for inference is high (not necessarily for multi-class learning), several methods have tried to alleviate this cost by, *e.g.*, using sparse methods [3] or more recently by assuming that the data lives around a linear subspace and then exploit a low-rank structure of the covariance matrix [8]. All these works, however, use several GPs for modeling the data, unlike the proposed method ETGP, and are hence expected to be more expensive.

5 Experiments

We evaluate ETGP in 5 UCI datasets [27] (see Fig. 3 for details). We compare ETGP with LINEAR, SAL and TANH flows with Bayesian (BA-ETGP) and point estimate (PE-ETGP) flow parameters predictions. We compare against a stationary independent (RBF), as described in Sec. 2.1, and dependent (RBF CORR) SVGPs, where dependencies are obtained by mixing C latent GPs [4]. We also compare against two non-stationary SVGP with an arccosine (ARCCOS) [11] and a Neural Network (NNET) [47] kernel. In SVGP, we run the model with separate/shared kernels and inducing points across classes, indicated with separate/shared K_ν in the results. We report accuracy (ACC) here. App. B contains log-likelihood (LL) results and gives all training details. We highlight that on each SVGP run (one per training hyperparameters), we pick the best result on the *test set*, so that the comparison with the ETGP is the most pessimistic. By contrast, we perform model selection with a validation set for ETGP. The code for ETGP will be released in Github.

5.1 Comparison against stationary dependent/independent SVGP

We compare ETGP against stationary dependent/independent SVGPs. The results obtained are displayed in Fig. 3. We observe that on the big datasets with a large number of classes (*i.e.*, `characterfont` and `devangari`) ETGP clearly outperforms SVGPs. In the worst case, the performance gain goes from 0.34 RBF CORR to 0.36 TANH. In the best case, we see a boost from 0.29 SVGP to 0.36 TANH both in `characterfont`. In `devangari` ETGPs are clearly better in all cases boosting accuracy from 0.93 RBF CORR to 0.96 TANH and LINEAR, nearly matching the result obtained by a convolutional neural network (0.98) [1]. This boost in performance is obtained around one order of magnitude faster, see Sec. 5.3 and Fig. 5. We also see that sharing inducing points and covariances (orange crosses) clearly drops performance. In `avila`, a medium size dataset, ETGP (0.985 TANH 0.970 LINEAR) works better than SVGP (0.962) and comparable to correlated SVGP (0.988), one order of magnitude faster.

In the small datasets (`vowel` and `absenteeism`) we observe different things. First on `vowel` SVGP sharing kernel and inducing points works best. This is because the training and test sets were collected from different speakers pronouncing vowels, and this domain shift can't be captured by these models. As a consequence, the shared K_ν model generalizes better since it under-fits the training set (reflected by worse ACC, LL and ELL in the training set), unlike separate K_ν and ETGP. Since ETGP chooses hyper-parameters using validation data extracted from the training set, this method cannot capture this domain shift. However, in some runs, ETGP (mostly those with higher dropout probability *i.e.* higher epistemic uncertainty) was able to match the results of SVGP with shared covariances. This remarks that epistemic uncertainty is beneficial in domain-shift small datasets, as expected. We emphasize that this is not a problem of the ETGP but derived from the characteristics of the dataset itself since it is also suffered by SVGP with separate K_ν . Note that on `absenteeism` (fewer training points than `vowel`) we see that the proposed model (0.307 LINEAR and 0.315 TANH) performs similarly to SVGP (0.314) and correlated SVGP (0.319). Finally, across all datasets, the SAL flow is the worst one (see App. B for possible explanations). We remark how well the C non-stationary dependent GPs (LINEAR) perform here, opening its use in other GP applications.

Regarding LL (see App. B), we observe similar results across all datasets. For small datasets BA-ETGP provides much better uncertainty quantification (LL), something we don't observe on the medium/large datasets in neither ACC or LL. This matches findings from [28] where being Bayesian

does not show improvements on classification datasets. This is expected as with big N epistemic uncertainty vanishes, suggesting that alternatives that fix the dropout probability depending on the number of training points, such as concrete dropout [16], are a potential line of research to enhance the proposed model.

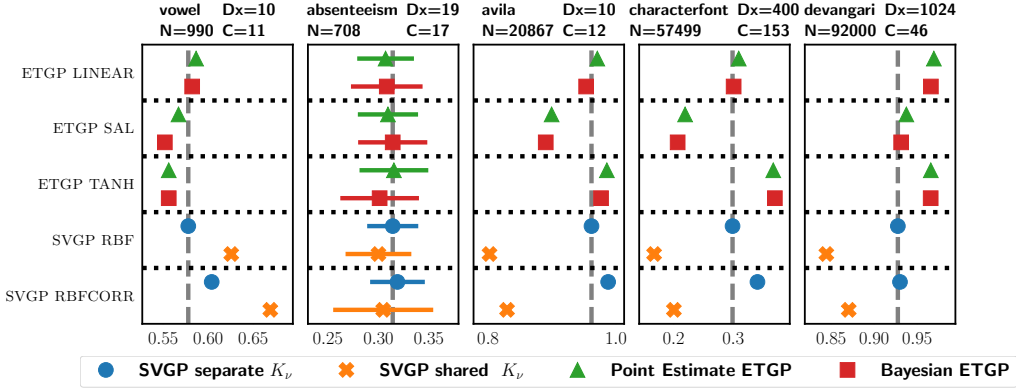


Figure 3: Avg. accuracy (right is better) comparing ETGP vs. independent/dependent stationary GPs.

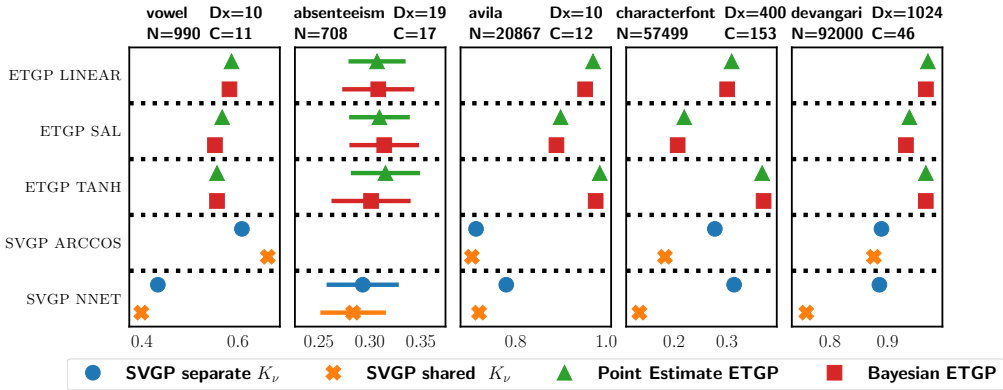


Figure 4: Avg. accuracy (right is better) comparing ETGP with two non-stationary GPs.

5.2 Comparison against Non-Stationary GP priors

We compare ETGP also against two non-stationary kernels Fig. 4. We observe that the NNET kernel often gives worse results than the ARCCOS or ETGP, especially for shared kernels across classes. This remarks the importance of having background knowledge about the non-stationarity of the particular application. Our work and [28] show that the non-stationarity achieved by input dependent flows is beneficial and easy to interpret since we just make each of the marginals depend directly on the part of the feature space that we are modeling, with no cross interactions between data points beyond those given by the base stationary kernel. ETGP outperforms both the NNET and ARCCOS kernel. In vowel, the shared SVGP kernel works the best, matching the results of Sec. 5.1. In terms of LL our model also works consistently better. See App. B for details. We don't show results for ARCCOS on absenteeism as we found training runs to saturate numerically (using float64 precision).

5.3 Timing comparison

We report the average training time in Fig. 5 and prediction time in App. B. By using MCDROP, the training time of the PE-ETGP and BA-ETGP is the same. Predictions for the Bayesian ETGPs can be computed in parallel. We refactorize GPFLOW's source code so that the shared SVGP model is more efficient, see App. C. We observe that ETGP is the fastest method, with a gain of one order of magnitude, compared to SVGP. SVGP with shared K_v is competitive in terms of training time, but has a drop in performance (see Sec. 5.1), unlike ETGP which typically performs best.

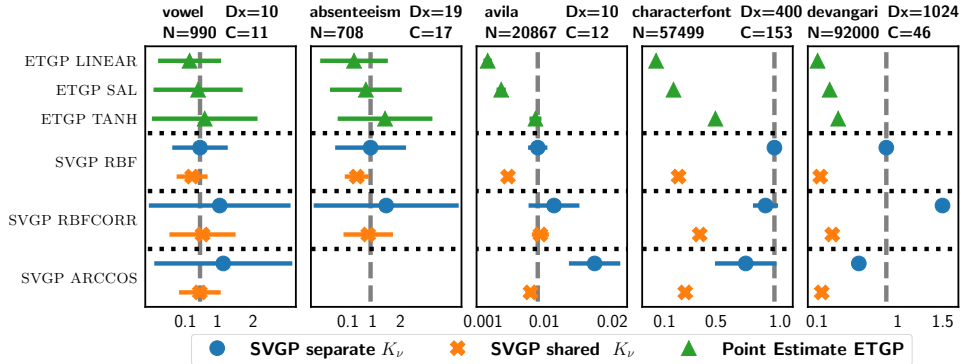


Figure 5: Average training time per epoch in minutes (left is better) comparing ETGP with SVGPs. NNET kernel is omitted as it is slower. Times for `absenteeism` and `vowel` are scaled by 10^3 .

5.4 Fewer inducing points act as a regularizer

In [28] it is shown that TGPs could match SVGPs performance in regression problems using 20 times less inducing points. We additionally found that using fewer inducing points can serve also as a regularizer, since the GP posterior is expected to parameterize smoother functions in that case. With this goal, we report results for ETGP using 50 and 100 inducing points, see Fig. 6. We observed that ETGP gets regularized when using fewer inducing points. In `vowel` it improves results, and matches SVGPs performance in `avila` and `absenteeism`. We extend this analysis in App. B.

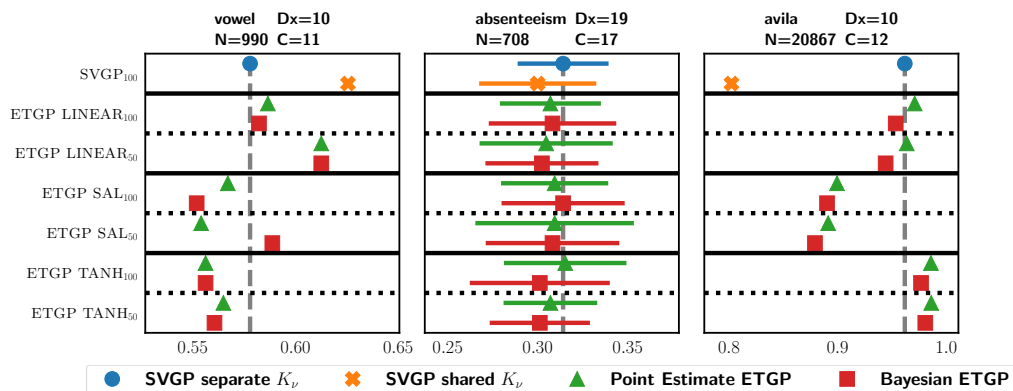


Figure 6: Results comparing ACC (right is better) using less inducing points.

6 Conclusions and future work

We have introduced the Efficient Transformed Gaussian Process (ETGP), as a way of creating C dependent non-stationary stochastic processes in an efficient way. For this, a single initial GP is transformed C times. This has the benefit of reducing the computational cost while providing enough model flexibility to learn complex tasks. We have provided an efficient training algorithm for ETGP based on variational inference. This method has been evaluated in the context of multi-class classification. Our results show that ETGP is competitive or even better than typical sparse SVGPs, at a lower computational cost. A limitation of ETGP is, however, that it leads to a model that is more difficult to interpret than SVGPs as a consequence of the non-linear transformations, although some flows allow controlling the moments of the induced distributions [34]. Future work can focus on extending ETGP to multi-task and multi-label problems, where a large number of processes is also needed, and its use in a deep kernel learning framework [49]. Also, an analysis of how the dependencies are modeled by sharing the copula of the base GP, including how additional dependencies can be gained by mixing ETGPs with a mixing matrix. The use of concrete dropout and using GPs instead of NNs to parameterize the flows are alternatives to improve different aspects of the Bayesian nature of the flow such as computational performance, well-specified Bayesian priors and epistemic uncertainty.

Acknowledgments and Disclosure of Funding

The authors acknowledge funding coming from the Spanish National Research Project PID2019-106827GB-I00. We also acknowledge the use of the computational resources from Centro de Computación Científica (CCC) and the AUDIAS Laboratory both at Universidad Autónoma de Madrid. Part of this work was carried out while J.M. was at the PRHLT research center at Universidad Politécnica de Valencia.

References

- [1] Acharya, S., Pant, A. K., and Gyawali, P. K. (2015). Deep learning based large scale handwritten Devanagari character recognition. *2015 9th International Conference on Software, Knowledge, Information Management and Applications (SKIMA)*, pages 1–6.
- [2] Adams, R. P. and Stegle, O. (2008). Gaussian process product models for nonparametric nonstationarity. In *Proceedings of the 25th International Conference on Machine Learning*, page 1–8.
- [3] Alvarez, M. and Lawrence, N. (2008). Sparse convolved Gaussian processes for multi-output regression. In *Advances in Neural Information Processing Systems*, pages 57–64.
- [4] Álvarez, M. A., Rosasco, L., and Lawrence, N. D. (2012). Kernels for vector-valued functions: A review. *Found. Trends Mach. Learn.*, 4:195–266.
- [5] Bishop, C. M. (2007). *Pattern recognition and machine learning, 5th Edition*. Information science and statistics. Springer.
- [6] Blackford, L. S., Petitet, A., Pozo, R., Remington, K., Whaley, R. C., Demmel, J., Dongarra, J., Duff, I., Hammarling, S., Henry, G., et al. (2002). An updated set of basic linear algebra subprograms (BLAS). *ACM Transactions on Mathematical Software*, 28:135–151.
- [7] Boyle, P. and Frean, M. (2004). Dependent Gaussian processes. In *Advances in Neural Information Processing Systems*, pages 217–224.
- [8] Bruinsma, W., Perim, E., Tebbutt, W., Hosking, S., Solin, A., and Turner, R. (2020). Scalable exact inference in multi-output Gaussian processes. In *Proceedings of the 37th International Conference on Machine Learning*, pages 1190–1201.
- [9] Calandra, R., Peters, J., Rasmussen, C. E., and Deisenroth, M. P. (2016). Manifold Gaussian processes for regression. In *2016 International Joint Conference on Neural Networks (IJCNN)*, pages 3338–3345.
- [10] Chai, K. M. A. (2012). Variational multinomial logit Gaussian process. *The Journal of Machine Learning Research*, 13:1745–1808.
- [11] Cho, Y. and Saul, L. (2009). Kernel methods for deep learning. In *Advances in Neural Information Processing Systems*, pages 342–350.
- [12] Damianou, A. and Lawrence, N. (2013). Deep Gaussian processes. In *Proceedings of the Sixteenth International Conference on Artificial Intelligence and Statistics*, pages 207–215.
- [13] Duvenaud, D., Lloyd, J., Grosse, R., Tenenbaum, J., and Zoubin, G. (2013). Structure discovery in nonparametric regression through compositional kernel search. In *International Conference on Machine Learning*, pages 1166–1174.
- [14] Gal, Y. (2016). *Uncertainty in Deep Learning*. PhD thesis, University of Cambridge.
- [15] Gal, Y. and Ghahramani, Z. (2016). Dropout as a Bayesian approximation: Representing model uncertainty in deep learning. In *Proceedings of the 33rd International Conference on International Conference on Machine Learning - Volume 48*, page 1050–1059.
- [16] Gal, Y., Hron, J., and Kendall, A. (2017). Concrete dropout. In *Advances in Neural Information Processing Systems*, volume 30, pages 3581–3590.
- [17] Gardner, J. R., Pleiss, G., Weinberger, K. Q., Bindel, D., and Wilson, A. G. (2018). Gpytorch: Blackbox matrix-matrix gaussian process inference with GPU acceleration. In *NeurIPS*, pages 7587–7597.
- [18] Hamelijnc, O., Damoulas, T., Wang, K., and Girolami, M. (2019). Multi-resolution multi-task Gaussian processes. In *Advances in Neural Information Processing Systems*, pages 14025–14035.

- [19] Heinonen, M., Mannerström, H., Rousu, J., Kaski, S., and Lähdesmäki, H. (2016). Non-stationary Gaussian process regression with Hamiltonian monte carlo. In *Proceedings of the 19th International Conference on Artificial Intelligence and Statistics*, pages 732–740.
- [20] Hensman, J., de G. Matthews, A. G., and Ghahramani, Z. (2015). Scalable variational gaussian process classification. In *AISTATS, JMLR Workshop and Conference Proceedings*.
- [21] Hensman, J., Fusi, N., and Lawrence, N. D. (2013). Gaussian processes for big data. In *Proceedings of the Twenty-Ninth Conference on Uncertainty in Artificial Intelligence*, page 282–290.
- [22] Jankowiak, M. and Gardner, J. (2019). Neural likelihoods for multi-output Gaussian processes.
- [23] Krige, D. G. (1951). *A statistical approach to some mine valuation and allied problems on the Witwatersrand: by DG Krige*. PhD thesis, University of the Witwatersrand.
- [24] Lawrence, N. (2003). Gaussian process latent variable models for visualisation of high dimensional data. In *Advances in neural information processing systems*, page 329–336.
- [25] Lázaro-Gredilla, M. and Figueiras-Vidal, A. (2009). Inter-domain Gaussian processes for sparse inference using inducing features. In *Advances in Neural Information Processing Systems 22*, pages 1087–1095.
- [26] Leimkuhler, B. and Matthews, C. (2015). *Molecular Dynamics: With Deterministic and Stochastic Numerical Methods*. Interdisciplinary Applied Mathematics. Springer International Publishing.
- [27] Lichman, M. (2013). UCI machine learning repository.
- [28] Maroñas, J., Hamelijnc, O., Knoblauch, J., and Damoulas, T. (2021). Transforming Gaussian processes with normalizing flows. In *Proceedings of The 24th International Conference on Artificial Intelligence and Statistics*, pages 1081–1089.
- [29] Matthews, A. G. d. G., van der Wilk, M., Nickson, T., Fujii, K., Boukouvalas, A., León-Villagrà, P., Ghahramani, Z., and Hensman, J. (2017). GPflow: A Gaussian process library using TensorFlow. *Journal of Machine Learning Research*, 18:1–6.
- [30] Neal, R. M. (1996). *Bayesian Learning for Neural Networks*. PhD thesis, University of Toronto.
- [31] Petersen, K. B. and Pedersen, M. S. (2012). The matrix cookbook. Version 20121115.
- [32] Rasmussen, C. E. and Williams, C. K. I. (2006). *Gaussian processes for machine learning*. Adaptive computation and machine learning. MIT Press.
- [33] Rios, G. (2020). Transport Gaussian processes for regression.
- [34] Rios, G. and Tobar, F. (2019). Compositionally-warped Gaussian processes. *Neural Networks*, 118:235–246.
- [35] Sampson, P. D. and Guttorp, P. (1992). Nonparametric estimation of nonstationary spatial covariance structure. *Journal of the American Statistical Association*, 87:pp. 108–119.
- [36] Schmidt, A. M., O’Hagan, A., and Schmidt, R. M. (2000). Bayesian inference for nonstationary spatial covariance structure via spatial deformations. *Journal of the Royal Statistical Society, Series B*, 65:745–758.
- [37] Sklar, A. (1959). Fonctions de répartition à n dimensions et leurs marges. *Publications de l’Institut de Statistique de l’Université de Paris*, 8:229–231.
- [38] Snelson, E. L., Rasmussen, C. E., and Ghahramani, Z. (2003). Warped gaussian processes. In *NIPS*, pages 337–344.
- [39] Snoek, J., Larochelle, H., and Adams, R. (2012). Practical Bayesian optimization of machine learning algorithms. In *Advances in neural information processing systems*, pages 2951–2959.
- [40] Snoek, J., Swersky, K., Zemel, R., and Adams, R. P. (2014). Input warping for Bayesian optimization of non-stationary functions. In *Proceedings of the 31st International Conference on Machine Learning - Volume 32*, page II–1674–II–1682.
- [41] Song, Y., Sohl-Dickstein, J., Kingma, D. P., Kumar, A., Ermon, S., and Poole, B. (2021). Score-based generative modeling through stochastic differential equations. In *International Conference on Learning Representations*.
- [42] Srivastava, N., Hinton, G., Krizhevsky, A., Sutskever, I., and Salakhutdinov, R. (2014). Dropout: A simple way to prevent neural networks from overfitting. *Journal of Machine Learning Research*, 15:1929–1958.

- [43] Titsias, M. (2009). Variational learning of inducing variables in sparse Gaussian processes. In *Proceedings of the Twelfth International Conference on Artificial Intelligence and Statistics*, pages 567–574.
- [44] Uhlenbeck, G. E. and Ornstein, L. S. (1930). On the theory of the Brownian motion. *Physical review*, 36:823.
- [45] van der Wilk, M., Dutordoir, V., John, S., Artemev, A., Adam, V., and Hensman, J. (2020). A framework for interdomain and multioutput Gaussian processes.
- [46] Wang, K., Hamelijnck, O., Damoulas, T., and Steel, M. (2020). Non-separable non-stationary random fields. In *Proceedings of the 37th International Conference on Machine Learning*, Proceedings of Machine Learning Research, pages 9887–9897.
- [47] Williams, C. (1996). Computing with infinite networks. In *Advances in Neural Information Processing Systems*, pages 295–301.
- [48] Wilson, A. G. and Ghahramani, Z. (2010). Copula processes. In Lafferty, J. D., Williams, C. K. I., Shawe-Taylor, J., Zemel, R. S., and Culotta, A., editors, *Advances in Neural Information Processing Systems 23*, pages 2460–2468.
- [49] Wilson, A. G., Hu, Z., Salakhutdinov, R., and Xing, E. P. (2016). Deep kernel learning. In *Proceedings of the 19th International Conference on Artificial Intelligence and Statistics*, pages 370–378.
- [50] Wilson, A. G., Knowles, D. A., and Ghahramani, Z. (2012). Gaussian process regression networks. In *Proceedings of the 29th International Conference on International Conference on Machine Learning*, page 1139–1146.
- [51] Yang, G. (2019). Wide feedforward or recurrent neural networks of any architecture are Gaussian processes. In *Advances in Neural Information Processing Systems*, pages 9947–9960.

Appendix for Efficient Transformed Gaussian Processes for Non-Stationary Dependent Multi-class Classification

A Math Appendix

In this appendix we provide a wider description of the equations involved in this paper, ranging from the model definition to the sparse variational inference algorithm. For completeness, and to make the improvements of the proposed model clearer, we start by describing the sparse variational inference algorithm applied to multi-class problems with and independent GP prior, previous to the definition of our model. Although we compare against correlated GPs using a mixing matrix, we don't provide its derivation since it goes beyond the scope of this appendix. In the end of this appendix we proof Prop. 1. If possible we keep all the conditioning set explicit in the equations presented.

A.1 Classification with independent GP priors

Given a classification problem with inputs $\mathbf{x} \in \mathcal{X} \subseteq \mathbb{R}^d$ and C outputs $y \in \mathcal{Y} \subset \mathbb{N}$, we want to learn C mapping functions from \mathbf{x} to the probability of belonging to each y ; given a set of observations $\mathcal{D} = \{\mathbf{x}^n, y^n\}_{n=1}^N$ with $\mathbf{X} = (\mathbf{x}^1, \dots, \mathbf{x}^N)$ and $\mathbf{y} = (y^1, \dots, y^N)$.

If this modeling procedure is done using GPs, then we place an independent GP on each of these C functions, each one parameterized by a mean function $\mu_\nu(\mathbf{x})$ (which we assume to be zero) and a covariance matrix $K_\nu^c(\mathbf{x}, \mathbf{x})$, parameterized by ν . Following the notation introduced in the main paper, the joint distribution of C processes at locations \mathbf{X} is given by:

$$p(\bar{\mathbf{f}}_0 | \bar{\nu}) = \prod_{c=1}^C \mathcal{N}(\mathbf{f}_0^c | \mathbf{0}, K_\nu^c(\mathbf{X}, \mathbf{X})) \quad (12)$$

where $\bar{\mathbf{f}}_0 = \{\mathbf{f}_0^1, \dots, \mathbf{f}_0^C\}$. This prior is combined with a likelihood $p(\mathbf{y} | \bar{\mathbf{f}}_0)$ that links latent functions to observations. In classification, a common choice is the Categorical Likelihood, giving the joint distribution:

$$p(\mathbf{y}, \bar{\mathbf{f}}_0) = p(\mathbf{y} | \bar{\mathbf{f}}_0)p(\bar{\mathbf{f}}_0) = \left[\prod_{n=1}^N \prod_{c=1}^C \pi_c(\bar{f}_{0,n}^c)^{\mathbb{I}(y^n=c)} \right] \prod_{c=1}^C \mathcal{N}(\mathbf{f}_0^c | \mathbf{0}, K_\nu^c(\mathbf{X}, \mathbf{X})), \quad (13)$$

where $\pi_c(\bar{f}_{0,n}^c) = \exp(f_0^c(\mathbf{x}^n)) / \sum_{c'=1}^C \exp(f_0^{c'}(\mathbf{x}^n))$ is the Softmax link function mapping latent vectors to probabilities, and $\mathbb{I}(\cdot)$ the indicator function.

In Bayesian learning, we are interested in the posterior $p(\bar{\mathbf{f}}_0 | \mathcal{D})$, which is intractable for many likelihoods, and computationally unfeasible since its complexity scales cubically with the number of training points. We now introduce the variational sparse derivation.

A.1.1 Variational sparse derivation

The idea behind sparse GPs is to use a set of M inducing points $\mathbf{z} \in \mathcal{X}$, with $\mathbf{Z} = (\mathbf{z}^1, \dots, \mathbf{z}^M)$, that acts as summary statistics of the data. Each inducing point \mathbf{z} has an associated latent value u_0 . Following the GP's prior definition, then at \mathbf{Z} we have $\mathbf{u}_0 \sim \text{GP}(\mathbf{u}_0 | \mathbf{0}, K_\nu(\mathbf{Z}, \mathbf{Z}))$. Thus, given \mathbf{X}, \mathbf{Z} the joint distribution is Gaussian given by:

$$p(\bar{\mathbf{f}}_0, \mathbf{u}_0 | \mathbf{X}, \mathbf{Z}, \nu) = \mathcal{N} \left(\begin{array}{c} \bar{\mathbf{f}}_0 \\ \mathbf{u}_0 \end{array} \middle| \begin{array}{cc} \mathbf{0} & K_\nu(\mathbf{X}, \mathbf{X}), K_\nu(\mathbf{X}, \mathbf{Z}) \\ \mathbf{0} & K_\nu(\mathbf{Z}, \mathbf{X}), K_\nu(\mathbf{Z}, \mathbf{Z}) \end{array} \right) \quad (14)$$

One key contribution from [43] is to define these inducing points to be variational parameters that are learned by minimizing the KLD between the approximate $q(\bar{\mathbf{f}}_0, \mathbf{u}_0)$ and true posterior

$p(\mathbf{f}_0, \mathbf{u}_0 \mid \mathcal{D}, \mathbf{Z}, \nu)$. Since \mathbf{z} do not belong to the model parameters, then they don't increase the model expressiveness hence protecting the learning procedure from overfitting.

The other key contribution from [43] is how the variational distribution is defined. In particular, $q(\mathbf{f}_0, \mathbf{u}_0) = p(\mathbf{f}_0 \mid \mathbf{u}_0)q(\mathbf{u}_0)$ so that the conditional's model prior $p(\mathbf{f}_0 \mid \mathbf{u}_0)$ gets canceled. Later, [21] propose to keep $q(\mathbf{u}_0 \mid \mathbf{m}, \mathbf{S})$ explicit by parameterizing it with a Gaussian distribution with parameters $\mathbf{m} \in \mathbb{R}^M$, $\mathbf{S} \in \mathbb{R}^{M \times M}$. With this, the ELBO can be optimized with stochastic variational inference.

If C independent GPs are going to be used, we can easily extend the presented equations as follows. The joint prior factorizes across C as above:

$$p(\bar{\mathbf{f}}_0, \bar{\mathbf{u}}_0 \mid \mathbf{X}, \bar{\mathbf{Z}}, \bar{\nu}) = \prod_{c=1}^C \mathcal{N} \left(\begin{array}{c} \mathbf{f}_0^c \\ \mathbf{u}_0^c \end{array} \middle| \begin{array}{c} \mathbf{0} \\ \mathbf{0} \end{array}, \begin{array}{cc} K_\nu^c(\mathbf{X}, \mathbf{X}), & K_\nu(\mathbf{X}, \mathbf{Z}^c) \\ K_\nu^c(\mathbf{Z}^c, \mathbf{X}), & K_\nu(\mathbf{Z}^c, \mathbf{Z}^c) \end{array} \right) \quad (15)$$

and the approximate posterior can be defined by factorizing across C as well:

$$q(\bar{\mathbf{f}}_0, \bar{\mathbf{u}}_0 \mid \mathbf{X}, \bar{\mathbf{Z}}, \bar{\nu}, \bar{\mathbf{m}}, \bar{\mathbf{S}}) = \prod_{c=1}^C p(\mathbf{f}_0^c \mid \mathbf{u}_0^c, \mathbf{X}, \mathbf{Z}^c, \nu_c) q(\mathbf{u}_0^c \mid \mathbf{m}^c, \mathbf{S}^c) \quad (16)$$

The KLD minimization between the approximate posterior and the true posterior is equivalent to maximizing the Evidence Lower Bound (ELBO), which we now derive:

$$\begin{aligned} \text{ELBO} &= \int_{\mathbf{f}_0^1} \dots \int_{\mathbf{f}_0^C} \int_{\mathbf{u}_0^1} \dots \int_{\mathbf{u}_0^C} q(\bar{\mathbf{f}}_0, \bar{\mathbf{u}}_0) \log \frac{p(\mathbf{y} \mid \bar{\mathbf{f}}_0) p(\bar{\mathbf{f}}_0, \bar{\mathbf{u}}_0)}{q(\bar{\mathbf{f}}_0, \bar{\mathbf{u}}_0)} d\mathbf{f}_0^1 \dots d\mathbf{f}_0^C d\mathbf{u}_0^1 \dots d\mathbf{u}_0^C \\ &= \underbrace{\int_{\mathbf{f}_0^1} \dots \int_{\mathbf{f}_0^C} \int_{\mathbf{u}_0^1} \dots \int_{\mathbf{u}_0^C} q(\bar{\mathbf{f}}_0, \bar{\mathbf{u}}_0) \log p(\mathbf{y} \mid \bar{\mathbf{f}}_0) d\mathbf{f}_0^1 \dots d\mathbf{f}_0^C d\mathbf{u}_0^1 \dots d\mathbf{u}_0^C}_{\text{ELL}} \\ &\quad + \underbrace{\int_{\mathbf{f}_0^1} \dots \int_{\mathbf{f}_0^C} \int_{\mathbf{u}_0^1} \dots \int_{\mathbf{u}_0^C} q(\bar{\mathbf{f}}_0, \bar{\mathbf{u}}_0) \log \frac{p(\bar{\mathbf{f}}_0, \bar{\mathbf{u}}_0)}{q(\bar{\mathbf{f}}_0, \bar{\mathbf{u}}_0)} d\mathbf{f}_0^1 \dots d\mathbf{f}_0^C d\mathbf{u}_0^1 \dots d\mathbf{u}_0^C}_{-\text{KLD}} \end{aligned} \quad (17)$$

where we have dropped the conditioning set for clarity. We now workout each term separately:

$$\begin{aligned} -\text{KLD} &= \int_{\mathbf{f}_0^1} \dots \int_{\mathbf{f}_0^C} \int_{\mathbf{u}_0^1} \dots \int_{\mathbf{u}_0^C} q(\bar{\mathbf{f}}_0, \bar{\mathbf{u}}_0) \log \frac{p(\bar{\mathbf{f}}_0, \bar{\mathbf{u}}_0)}{q(\bar{\mathbf{f}}_0, \bar{\mathbf{u}}_0)} d\mathbf{f}_0^1 \dots d\mathbf{f}_0^C d\mathbf{u}_0^1 \dots d\mathbf{u}_0^C \\ &= \int_{\mathbf{u}_0^1} \dots \int_{\mathbf{u}_0^C} q(\bar{\mathbf{u}}_0) \log \frac{p(\bar{\mathbf{f}}_0 \mid \bar{\mathbf{u}}_0) p(\bar{\mathbf{u}}_0)}{p(\bar{\mathbf{f}}_0 \mid \bar{\mathbf{u}}_0) q(\bar{\mathbf{u}}_0)} d\mathbf{u}_0^1 \dots d\mathbf{u}_0^C \\ &= \int_{\mathbf{u}_0^1} \dots \int_{\mathbf{u}_0^C} \prod_{c=1}^C q(\mathbf{u}_0^c) \sum_{c'=1}^C \log \frac{p(\mathbf{u}_0^{c'})}{q(\mathbf{u}_0^{c'})} d\mathbf{u}_0^1 \dots d\mathbf{u}_0^C = \\ &= \sum_{c'=1}^C \int_{\mathbf{u}_0^1} \dots \int_{\mathbf{u}_0^C} \prod_{c=1}^C q(\mathbf{u}_0^c) \log \frac{p(\mathbf{u}_0^{c'})}{q(\mathbf{u}_0^{c'})} d\mathbf{u}_0^1 \dots d\mathbf{u}_0^C = \\ &= \sum_{c=1}^C \int_{\mathbf{u}_0^c} q(\mathbf{u}_0^c) \log \frac{p(\mathbf{u}_0^c)}{q(\mathbf{u}_0^c)} d\mathbf{u}_0^c \\ &= - \sum_{c=1}^C \text{KLD}[q(\mathbf{u}_0^c) \parallel p(\mathbf{u}_0^c)] \end{aligned} \quad (18)$$

The Expected log likelihood (ELL) is given by:

$$\begin{aligned}
\text{ELL} &= \int_{\mathbf{f}_0^1} \dots \int_{\mathbf{f}_0^C} \int_{\mathbf{u}_0^1} \dots \int_{\mathbf{u}_0^C} q(\bar{\mathbf{f}}_0, \bar{\mathbf{u}}_0) \log p(\mathbf{y} \mid \bar{\mathbf{f}}_0) d\mathbf{f}_0^1 \dots d\mathbf{f}_0^C d\mathbf{u}_0^1 \dots d\mathbf{u}_0^C \\
&= \int_{\mathbf{f}_0^1} \dots \int_{\mathbf{f}_0^C} q(\bar{\mathbf{f}}_0) \log \prod_{n=1}^N p(y^n \mid \bar{f}_{0,n}) d\mathbf{f}_0^1 \dots d\mathbf{f}_0^C \\
&= \int_{\mathbf{f}_0^1} \dots \int_{\mathbf{f}_0^C} q(\mathbf{f}_0^1) \dots q(\mathbf{f}_0^C) \log \prod_{n=1}^N \prod_{c=1}^C \pi_c(\bar{f}_{0,n}) \mathbb{I}(y^n=c) d\mathbf{f}_0^1 \dots d\mathbf{f}_0^C \\
&= \sum_{n=1}^N \sum_{c=1}^C \mathbb{I}(y^n=c) \int_{f_{0,n}^1} \dots \int_{f_{0,n}^C} q(f_{0,n}^1) \dots q(f_{0,n}^C) \log \pi_c(\bar{f}_{0,n}) df_{0,n}^1 \dots df_{0,n}^C
\end{aligned} \tag{19}$$

recovering the bound of the main paper (Eq. 2):

$$\begin{aligned}
\text{ELBO} &= \sum_{n=1}^N \sum_{c=1}^C \mathbb{I}(y^n=c) \int_{f_{0,n}^1} \dots \int_{f_{0,n}^C} q(f_{0,n}^1) \dots q(f_{0,n}^C) \log \pi_c(\bar{f}_{0,n}) df_{0,n}^1 \dots df_{0,n}^C \\
&\quad - \sum_{c=1}^C \text{KLD}[q(\mathbf{u}_0^c) \parallel p(\mathbf{u}_0^c)]
\end{aligned} \tag{20}$$

Note that this bound is amenable to stochastic optimization using minibatches, where the integrals are approximated by Monte Carlo using reparameterized gradients (a.k.a. path-wise gradients). The KLD can be computed in closed form. Most importantly, each $q(f_{0,n}^c)$ is a univariate Gaussian distribution given by:

$$\begin{aligned}
q(f_{0,n}^c) &= \mathcal{N}(f_{0,n}^c \mid K_{\nu \mathbf{x}^n, \mathbf{z}^c} K_{\nu \mathbf{z}^c, \mathbf{z}^c}^{-1} \mathbf{m}^c, \\
&\quad K_{\nu \mathbf{x}^n, \mathbf{x}^n} - K_{\nu \mathbf{x}^n, \mathbf{z}^c} K_{\nu \mathbf{z}^c, \mathbf{z}^c}^{-1} [K_{\nu \mathbf{z}^c, \mathbf{z}^c} + \mathbf{S}^c] K_{\nu \mathbf{z}^c, \mathbf{z}^c}^{-1} K_{\nu \mathbf{z}^c, \mathbf{x}^n})
\end{aligned} \tag{21}$$

obtained by solving $\int_{\mathbf{u}_0^1} \dots \int_{\mathbf{u}_0^C} \prod_{c=1}^C p(\mathbf{f}_0^c \mid \mathbf{u}_0^c, \mathbf{X}, \mathbf{Z}^c, \nu_c) q(\mathbf{u}_0^c \mid \mathbf{m}^c, \mathbf{S}^c) d\mathbf{u}_0^1 \dots d\mathbf{u}_0^C = \prod_{c=1}^C \int_{\mathbf{u}_0^c} p(\mathbf{f}_0^c \mid \mathbf{u}_0^c, \mathbf{X}, \mathbf{Z}^c, \nu_c) q(\mathbf{u}_0^c \mid \mathbf{m}^c, \mathbf{S}^c) d\mathbf{u}_0^c$. This computation needs to be computed C times requiring a complexity of $\mathcal{O}(CM^3 + CNM^2)$, which can be reduced to $\mathcal{O}(M^3 + CNM^2)$ if the inducing points are shared. We can gain additional performance if the kernel is shared as noted in App. C. However, as shown in the experiments sharing kernel and inducing points can drop performance.

A.2 Classification with Efficient Transformed Gaussian Processes

We now present the derivations required for the proposed model. This model is specified by transforming a single sample from a GP using C invertible transformations \mathbb{G}_{θ_K} by the following generative procedure:

$$\begin{aligned}
f_0(\cdot) &\sim \text{GP}(0, K_\nu(\cdot, \cdot)) \\
f_K^1(\cdot) &= \mathbb{G}_{\theta_K}^1(\mathbf{w}^1, \mathbf{X})(f_0(\cdot)), \dots, f_K^C(\cdot) = \mathbb{G}_{\theta_K}^C(\mathbf{w}^C, \mathbf{X})(f_0(\cdot)).
\end{aligned} \tag{22}$$

The prior distribution over C processes is derived as follows. For exemplification purposes consider $C = 3$ and consider the processes evaluation at the index set \mathbf{X} , then we have:

$$\begin{aligned}
\mathbf{f}_0 &\sim p(\mathbf{f}_0 \mid \mathbf{X}, \nu) \\
\mathbf{f}_K^1 &= \mathbb{G}_{\theta_K}^1(\mathbf{w}^1, \mathbf{X})(\mathbf{f}_0); \mathbf{f}_K^1 = \mathbb{G}_{\theta_K}^1(\mathbf{w}^1, \mathbf{X}) \circ \mathbb{H}_{\theta_K}^2(\mathbf{w}^2, \mathbf{X})(\mathbf{f}_K^2); \mathbf{f}_K^1 = \mathbb{G}_{\theta_K}^1(\mathbf{w}^1, \mathbf{X}) \circ \mathbb{H}_{\theta_K}^3(\mathbf{w}^3, \mathbf{X})(\mathbf{f}_K^3) \\
\mathbf{f}_K^2 &= \mathbb{G}_{\theta_K}^2(\mathbf{w}^2, \mathbf{X})(\mathbf{f}_0); \mathbf{f}_K^2 = \mathbb{G}_{\theta_K}^2(\mathbf{w}^2, \mathbf{X}) \circ \mathbb{H}_{\theta_K}^1(\mathbf{w}^1, \mathbf{X})(\mathbf{f}_K^1); \mathbf{f}_K^2 = \mathbb{G}_{\theta_K}^2(\mathbf{w}^2, \mathbf{X}) \circ \mathbb{H}_{\theta_K}^3(\mathbf{w}^3, \mathbf{X})(\mathbf{f}_K^3) \\
\mathbf{f}_K^3 &= \mathbb{G}_{\theta_K}^3(\mathbf{w}^3, \mathbf{X})(\mathbf{f}_0); \mathbf{f}_K^3 = \mathbb{G}_{\theta_K}^3(\mathbf{w}^3, \mathbf{X}) \circ \mathbb{H}_{\theta_K}^1(\mathbf{w}^1, \mathbf{X})(\mathbf{f}_K^1); \mathbf{f}_K^3 = \mathbb{G}_{\theta_K}^3(\mathbf{w}^3, \mathbf{X}) \circ \mathbb{H}_{\theta_K}^2(\mathbf{w}^2, \mathbf{X})(\mathbf{f}_K^2)
\end{aligned} \tag{23}$$

with $\mathbb{H} := \mathbb{G}^{-1}$. In order to define the prior probability of the classes we first observe that the following conditional independence holds from the construction introduced above:

$$\begin{aligned}
p(\mathbf{f}_K^1, \mathbf{f}_K^2, \mathbf{f}_K^3) &= p(\mathbf{f}_K^1) p(\mathbf{f}_K^2 \mid \mathbf{f}_K^1) p(\mathbf{f}_K^3 \mid \mathbf{f}_K^1, \cancel{\mathbf{f}_K^2}) \\
p(\mathbf{f}_K^2, \mathbf{f}_K^1, \mathbf{f}_K^3) &= p(\mathbf{f}_K^2) p(\mathbf{f}_K^1 \mid \mathbf{f}_K^2) p(\mathbf{f}_K^3 \mid \mathbf{f}_K^2, \cancel{\mathbf{f}_K^1}) \\
p(\mathbf{f}_K^3, \mathbf{f}_K^1, \mathbf{f}_K^2) &= p(\mathbf{f}_K^3) p(\mathbf{f}_K^1 \mid \mathbf{f}_K^3) p(\mathbf{f}_K^2 \mid \mathbf{f}_K^3, \cancel{\mathbf{f}_K^1})
\end{aligned} \tag{24}$$

where we have chosen to write the 3 out of 6 possibilities just for exemplification purposes. This conditional independence holds because the probability of \mathbf{f}_K^3 given $\mathbf{f}_K^1, \mathbf{f}_K^2$ is given by a direct mapping either from \mathbf{f}_K^1 or \mathbf{f}_K^2 as illustrated in Eq. 23. We define the *pivot* to be the member on which we *always* condition, i.e. if $p(\mathbf{f}_K^3 | \mathbf{f}_K^2, \mathbf{f}_K^1) = p(\mathbf{f}_K^3 | \mathbf{f}_K^1)$ then the *pivot* is \mathbf{f}_K^1 . Note, however, that it will also be valid to choose any other member as a *pivot*, for example $p(\mathbf{f}_K^3 | \mathbf{f}_K^2, \mathbf{f}_K^1) = p(\mathbf{f}_K^3 | \mathbf{f}_K^2)$. Finally, note that we can write the conditional distribution $p(\mathbf{f}_K^3 | \mathbf{f}_K^1)$ as:

$$p(\mathbf{f}_K^3 | \mathbf{f}_K^1) = \delta \left(\mathbf{f}_K^3 - \mathbb{G}_{\theta_K}^3(\mathbf{w}^3, \mathbf{x}) \circ \mathbb{H}_{\theta_K}^1(\mathbf{w}^1, \mathbf{x})(\mathbf{f}_K^1) \right) \quad (25)$$

with δ being the Dirac delta measure. Using both observations we can write the prior joint conditional distribution over the classes as:

$$p(\bar{\mathbf{f}}_K | \bar{\mathbb{G}}_{\theta_K}, \bar{\mathbf{W}}, \mathbf{X}, \nu) = p(\mathbf{f}_0 | \mathbf{X}, \nu) \prod_{k=0}^{K^1-1} \left| \det \frac{\partial \mathbb{G}_{\theta_k}^1(\mathbf{w}^1, \mathbf{x})(\mathbf{f}_K^1)}{\partial \mathbf{f}_K^1} \right|^{-1} \quad (26)$$

$$\prod_{c=2}^C \delta \left(\mathbf{f}_K^c - \mathbb{G}_{\theta_K}^c(\mathbf{w}^c, \mathbf{x}) \circ \mathbb{H}_{\theta_K}^1(\mathbf{w}^1, \mathbf{x})(\mathbf{f}_K^1) \right)$$

recovering the expression in Eq. 6 in the main paper. The overall joint is given by:

$$p(\bar{\mathbf{f}}_K, \bar{\mathbf{W}} | \bar{\mathbb{G}}_{\theta_K}, \bar{\lambda}, \mathbf{X}, \nu) = p(\bar{\mathbf{f}}_K | \bar{\mathbb{G}}_{\theta_K}, \bar{\mathbf{W}}, \mathbf{X}, \nu) p(\bar{\mathbf{W}} | \bar{\lambda}) \quad (27)$$

with $p(\bar{\mathbf{W}} | \bar{\lambda})$ denoting the prior over the parameters of the Bayesian Neural Network (BNN).

A.2.1 Prior conditional distribution $p(\bar{\mathbf{f}}_K | \bar{\mathbf{u}}_K)$

We now derive the prior conditional distribution $p(\bar{\mathbf{f}}_K | \bar{\mathbf{u}}_K)$. In a similar vein to GPs we will derive a sparse variational inference algorithm, from where inducing points need to be incorporated. Note that since we use diagonal flows, the resulting joint distribution is consistent (i.e. is a finite dimensional realization of a stochastic process), which means we can extend its index set introducing inducing points $\bar{\mathbf{u}}_K$ at inducing locations \mathbf{Z} , similar to what we do in GPs.

First, note that following the previous section we can write the marginal distribution at the inducing points by:

$$p(\bar{\mathbf{u}}_K | \bar{\mathbb{G}}_{\theta_K}, \bar{\mathbf{W}}, \mathbf{Z}, \nu) = p(\mathbf{u}_0 | \mathbf{Z}, \nu) \prod_{k=0}^{K^1-1} \left| \det \frac{\partial \mathbb{G}_{\theta_k}^1(\mathbf{w}^1, \mathbf{z})(\mathbf{u}_K^1)}{\partial \mathbf{u}_K^1} \right|^{-1} \quad (28)$$

$$\prod_{c=2}^C \delta \left(\mathbf{u}_K^c - \mathbb{G}_{\theta_K}^c(\mathbf{w}^c, \mathbf{z}) \circ \mathbb{H}_{\theta_K}^1(\mathbf{w}^1, \mathbf{z})(\mathbf{u}_K^1) \right).$$

The overall joint can be derived following a similar procedure. Note that we have:

$$\mathbf{f}_0, \mathbf{u}_0 \sim p(\mathbf{f}_0, \mathbf{u}_0 | \mathbf{X}, \mathbf{Z}, \lambda)$$

$$\begin{aligned} \mathbf{f}_K^1 &= \mathbb{G}_{\theta_K}^1(\mathbf{w}^1, \mathbf{x})(\mathbf{f}_0); & \mathbf{f}_K^1 &= \mathbb{G}_{\theta_K}^1(\mathbf{w}^1, \mathbf{x}) \circ \mathbb{H}_{\theta_K}^2(\mathbf{w}^2, \mathbf{x})(\mathbf{f}_K^2); & \mathbf{f}_K^1 &= \mathbb{G}_{\theta_K}^1(\mathbf{w}^1, \mathbf{x}) \circ \mathbb{H}_{\theta_K}^3(\mathbf{w}^3, \mathbf{x})(\mathbf{f}_K^3) \\ \mathbf{u}_K^1 &= \mathbb{G}_{\theta_K}^1(\mathbf{w}^1, \mathbf{z})(\mathbf{u}_0); & \mathbf{u}_K^1 &= \mathbb{G}_{\theta_K}^1(\mathbf{w}^1, \mathbf{z}) \circ \mathbb{H}_{\theta_K}^2(\mathbf{w}^2, \mathbf{z})(\mathbf{u}_K^2); & \mathbf{u}_K^1 &= \mathbb{G}_{\theta_K}^1(\mathbf{w}^1, \mathbf{z}) \circ \mathbb{H}_{\theta_K}^3(\mathbf{w}^3, \mathbf{z})(\mathbf{u}_K^3) \\ \mathbf{f}_K^2 &= \mathbb{G}_{\theta_K}^2(\mathbf{w}^2, \mathbf{x})(\mathbf{f}_0); & \mathbf{f}_K^2 &= \mathbb{G}_{\theta_K}^2(\mathbf{w}^2, \mathbf{x}) \circ \mathbb{H}_{\theta_K}^1(\mathbf{w}^1, \mathbf{x})(\mathbf{f}_K^1); & \mathbf{f}_K^2 &= \mathbb{G}_{\theta_K}^2(\mathbf{w}^2, \mathbf{x}) \circ \mathbb{H}_{\theta_K}^3(\mathbf{w}^3, \mathbf{x})(\mathbf{f}_K^3) \\ \mathbf{u}_K^2 &= \mathbb{G}_{\theta_K}^2(\mathbf{w}^2, \mathbf{z})(\mathbf{u}_0); & \mathbf{u}_K^2 &= \mathbb{G}_{\theta_K}^2(\mathbf{w}^2, \mathbf{z}) \circ \mathbb{H}_{\theta_K}^1(\mathbf{w}^1, \mathbf{z})(\mathbf{u}_K^1); & \mathbf{u}_K^2 &= \mathbb{G}_{\theta_K}^2(\mathbf{w}^2, \mathbf{z}) \circ \mathbb{H}_{\theta_K}^3(\mathbf{w}^3, \mathbf{z})(\mathbf{u}_K^3) \\ \mathbf{f}_K^3 &= \mathbb{G}_{\theta_K}^3(\mathbf{w}^3, \mathbf{x})(\mathbf{f}_0); & \mathbf{f}_K^3 &= \mathbb{G}_{\theta_K}^3(\mathbf{w}^3, \mathbf{x}) \circ \mathbb{H}_{\theta_K}^1(\mathbf{w}^1, \mathbf{x})(\mathbf{f}_K^1); & \mathbf{f}_K^3 &= \mathbb{G}_{\theta_K}^3(\mathbf{w}^3, \mathbf{x}) \circ \mathbb{H}_{\theta_K}^2(\mathbf{w}^2, \mathbf{x})(\mathbf{f}_K^2) \\ \mathbf{u}_K^3 &= \mathbb{G}_{\theta_K}^3(\mathbf{w}^3, \mathbf{z})(\mathbf{u}_0); & \mathbf{u}_K^3 &= \mathbb{G}_{\theta_K}^3(\mathbf{w}^3, \mathbf{z}) \circ \mathbb{H}_{\theta_K}^1(\mathbf{w}^1, \mathbf{z})(\mathbf{u}_K^1); & \mathbf{u}_K^3 &= \mathbb{G}_{\theta_K}^3(\mathbf{w}^3, \mathbf{z}) \circ \mathbb{H}_{\theta_K}^2(\mathbf{w}^2, \mathbf{z})(\mathbf{u}_K^2) \end{aligned}$$

Following similar ideas as before, the pivots are now defined to be \mathbf{f}_K^1 and \mathbf{u}_K^1 . We can also apply a similar conditional independence, and note that the joint distribution over the non *pivots* $\mathbf{f}_K, \mathbf{u}_K$ also factorizes. Conditional independence holds because any $\mathbf{f}_K^c, \mathbf{u}_K^c$ only depends on $\mathbf{f}_K^1, \mathbf{u}_K^1$ by a direct mapping; and the conditional distribution over the non *pivots* $p(\mathbf{f}_K^c, \mathbf{u}_K^c | \mathbf{f}_K^1, \mathbf{u}_K^1) = p(\mathbf{f}_K^c |$

$\mathbf{f}_K^1)p(\mathbf{u}_K^c | \mathbf{u}_K^1)$ factorizes since \mathbf{f}_K^c only depends on \mathbf{f}_K^1 and \mathbf{u}_K^c on \mathbf{u}_K^1 . Writing:

$$\begin{aligned}
& p(\mathbf{f}_K^1, \mathbf{u}_K^1, \mathbf{f}_K^2, \mathbf{u}_K^2, \mathbf{f}_K^3, \mathbf{u}_K^3) = \\
& p(\mathbf{f}_K^1, \mathbf{u}_K^1)p(\mathbf{f}_K^2, \mathbf{u}_K^2 | \mathbf{f}_K^1, \mathbf{u}_K^1)p(\mathbf{f}_K^3, \mathbf{u}_K^3 | \mathbf{f}_K^1, \mathbf{u}_K^1, \mathbf{f}_K^2, \mathbf{u}_K^2) = \\
& p(\mathbf{f}_K^1, \mathbf{u}_K^1)p(\mathbf{f}_K^2 | \mathbf{f}_K^1)p(\mathbf{u}_K^2 | \mathbf{u}_K^1)p(\mathbf{f}_K^3 | \mathbf{f}_K^1)p(\mathbf{u}_K^3 | \mathbf{u}_K^1) = \\
& \underbrace{p(\mathbf{f}_0 | \mathbf{u}_0) \prod_{k=0}^{K^1-1} \left| \det \frac{\partial \mathbb{G}_{\theta_k}^1(\mathbf{w}^1, \mathbf{x})(\mathbf{f}_K^1)}{\partial \mathbf{f}_K^1} \right|^{-1}}_{p(\mathbf{f}_K^1 | \mathbf{u}_K^1)} \underbrace{p(\mathbf{u}_0) \prod_{k=0}^{K^1-1} \left| \det \frac{\partial \mathbb{G}_{\theta_k}^1(\mathbf{w}^1, \mathbf{z})(\mathbf{u}_K^1)}{\partial \mathbf{u}_K^1} \right|^{-1}}_{p(\mathbf{u}_K^1)} \\
& \underbrace{\delta \left(\mathbf{f}_K^2 - \mathbb{G}_{\theta_K}^2(\mathbf{w}^2, \mathbf{x}) \circ \mathbb{H}_{\theta_K}^1(\mathbf{w}^1, \mathbf{x})(\mathbf{f}_K^1) \right)}_{p(\mathbf{f}_K^2, \mathbf{u}_K^2 | \mathbf{f}_K^1, \mathbf{u}_K^1) = p(\mathbf{f}_K^2 | \mathbf{f}_K^1)p(\mathbf{u}_K^2 | \mathbf{u}_K^1)} \delta \left(\mathbf{u}_K^2 - \mathbb{G}_{\theta_K}^2(\mathbf{w}^2, \mathbf{z}) \circ \mathbb{H}_{\theta_K}^1(\mathbf{w}^1, \mathbf{z})(\mathbf{u}_K^1) \right) \\
& \underbrace{\delta \left(\mathbf{f}_K^3 - \mathbb{G}_{\theta_K}^3(\mathbf{w}^3, \mathbf{x}) \circ \mathbb{H}_{\theta_K}^1(\mathbf{w}^1, \mathbf{x})(\mathbf{f}_K^1) \right)}_{p(\mathbf{f}_K^3, \mathbf{u}_K^3 | \mathbf{f}_K^1, \mathbf{u}_K^1) = p(\mathbf{f}_K^3 | \mathbf{f}_K^1)p(\mathbf{u}_K^3 | \mathbf{u}_K^1)} \delta \left(\mathbf{u}_K^3 - \mathbb{G}_{\theta_K}^3(\mathbf{w}^3, \mathbf{z}) \circ \mathbb{H}_{\theta_K}^1(\mathbf{w}^1, \mathbf{z})(\mathbf{u}_K^1) \right)
\end{aligned} \tag{29}$$

Because we use a diagonal flow, the full Jacobian factorizes as $\prod_{k=0}^{K^1-1} \left| \det \frac{\partial \mathbb{G}_{\theta_k}^1(\mathbf{w}^1, \mathbf{x})(\mathbf{f}_K^1)}{\partial \mathbf{f}_K^1} \right|^{-1} \prod_{k=0}^{K^1-1} \left| \det \frac{\partial \mathbb{G}_{\theta_k}^1(\mathbf{w}^1, \mathbf{z})(\mathbf{u}_K^1)}{\partial \mathbf{u}_K^1} \right|^{-1}$, allowing us to explicitly write $p(\mathbf{f}_K^1 | \mathbf{u}_K^1)$ and $p(\mathbf{u}_K^1)$ (see appendix of [28]). Thus, the overall joint distribution is given by:

$$\begin{aligned}
p(\bar{\mathbf{f}}_K, \bar{\mathbf{u}}_K, \bar{\mathbf{W}} | \bar{\mathbb{G}}_{\theta_K}, \mathbf{X}, \mathbf{Z}, \bar{\lambda}, \nu) &= \prod_{c=1}^C p(\mathbf{W}^c | \lambda^c) \\
& \underbrace{p(\mathbf{f}_0 | \mathbf{u}_0, \mathbf{X}, \mathbf{Z}, \nu) \prod_{k=0}^{K^1-1} \left| \det \frac{\partial \mathbb{G}_{\theta_k}^1(\mathbf{w}^1, \mathbf{x})(\mathbf{f}_K^1)}{\partial \mathbf{f}_K^1} \right|^{-1} \prod_{c=2}^C \delta \left(\mathbf{f}_K^c - \mathbb{G}_{\theta_K}^c(\mathbf{w}^c, \mathbf{x}) \circ \mathbb{H}_{\theta_K}^1(\mathbf{w}^1, \mathbf{x})(\mathbf{f}_K^1) \right)}_{p(\bar{\mathbf{f}}_K | \bar{\mathbf{u}}_K)} \\
& \underbrace{p(\mathbf{u}_0 | \mathbf{Z}, \nu) \prod_{k=0}^{K^1-1} \left| \det \frac{\partial \mathbb{G}_{\theta_k}^1(\mathbf{w}^1, \mathbf{z})(\mathbf{u}_K^1)}{\partial \mathbf{u}_K^1} \right|^{-1} \prod_{c=2}^C \delta \left(\mathbf{u}_K^c - \mathbb{G}_{\theta_K}^c(\mathbf{w}^c, \mathbf{z}) \circ \mathbb{H}_{\theta_K}^1(\mathbf{w}^1, \mathbf{z})(\mathbf{u}_K^1) \right)}_{p(\bar{\mathbf{u}}_K)}
\end{aligned} \tag{30}$$

where now the *pivots* are \mathbf{u}_K^1 and \mathbf{f}_K^1 . To fully characterize the joint distribution we shall derive where the expression for $p(\bar{\mathbf{f}}_K | \bar{\mathbf{u}}_K)$ in Eq. 30 comes from. This conditional distribution is derived by inspection as follows. We factorize the joint distribution in the following two equivalent ways:

$$\begin{aligned}
& p(\mathbf{f}_K^1, \mathbf{f}_K^2, \mathbf{f}_K^3, \mathbf{u}_K^1, \mathbf{u}_K^2, \mathbf{u}_K^3) = \\
& p(\mathbf{f}_K^1, \mathbf{f}_K^2, \mathbf{f}_K^3 | \mathbf{u}_K^1, \mathbf{u}_K^2, \mathbf{u}_K^3)p(\mathbf{u}_K^1, \mathbf{u}_K^2, \mathbf{u}_K^3) = \\
& p(\mathbf{f}_K^1, \mathbf{u}_K^1)p(\mathbf{f}_K^2, \mathbf{u}_K^2 | \mathbf{u}_K^1, \mathbf{u}_K^1)p(\mathbf{f}_K^3, \mathbf{u}_K^3 | \mathbf{f}_K^1, \mathbf{u}_K^1)
\end{aligned}$$

and used the form of the third line, which is the one we know how to write (Eq. 29), to derive the expression for the second line, which is the object of our interest. The expression for the third line

has already been written and is given by:

$$\begin{aligned}
& p(\mathbf{f}_K^1, \mathbf{f}_K^2, \mathbf{f}_K^3, \mathbf{u}_K^1, \mathbf{u}_K^2, \mathbf{u}_K^3) = \\
& \underbrace{p(\mathbf{f}_0 | \mathbf{u}_0) p(\mathbf{u}_0) \prod_{k=0}^{K^1-1} \left| \det \frac{\partial \mathbb{G}_{\theta_k}^1(\mathbf{w}^1, \mathbf{x})(\mathbf{f}_K^1)}{\partial \mathbf{f}_K^1} \right|^{-1} \prod_{k=0}^{K^1-1} \left| \det \frac{\partial \mathbb{G}_{\theta_k}^1(\mathbf{w}^1, \mathbf{z})(\mathbf{u}_K^1)}{\partial \mathbf{u}_K^1} \right|^{-1}}_{p(\mathbf{f}_K^1, \mathbf{u}_K^1)} \\
& \underbrace{\delta \left(\mathbf{f}_K^2 - \mathbb{G}_{\theta_K}^2(\mathbf{w}^2, \mathbf{x}) \circ \mathbb{H}_{\theta_K}^1(\mathbf{w}^1, \mathbf{x})(\mathbf{f}_K^1) \right) \delta \left(\mathbf{u}_K^2 - \mathbb{G}_{\theta_K}^2(\mathbf{w}^2, \mathbf{z}) \circ \mathbb{H}_{\theta_K}^1(\mathbf{w}^1, \mathbf{z})(\mathbf{u}_K^1) \right)}_{p(\mathbf{f}_K^2, \mathbf{u}_K^2 | \mathbf{f}_K^1, \mathbf{u}_K^1)} \\
& \underbrace{\delta \left(\mathbf{f}_K^3 - \mathbb{G}_{\theta_K}^3(\mathbf{w}^3, \mathbf{x}) \circ \mathbb{H}_{\theta_K}^1(\mathbf{w}^1, \mathbf{x})(\mathbf{f}_K^1) \right) \delta \left(\mathbf{u}_K^3 - \mathbb{G}_{\theta_K}^3(\mathbf{w}^3, \mathbf{z}) \circ \mathbb{H}_{\theta_K}^1(\mathbf{w}^1, \mathbf{z})(\mathbf{u}_K^1) \right)}_{p(\mathbf{f}_K^3, \mathbf{u}_K^3 | \mathbf{f}_K^1, \mathbf{u}_K^1)}
\end{aligned} \tag{31}$$

Then, since we know the form of $p(\mathbf{u}_K^1, \mathbf{u}_K^2, \mathbf{u}_K^3)$:

$$\begin{aligned}
& p(\mathbf{u}_K^1, \mathbf{u}_K^2, \mathbf{u}_K^3) = \\
& p(\mathbf{u}_0) \prod_{k=0}^{K^1-1} \left| \det \frac{\partial \mathbb{G}_{\theta_k}^1(\mathbf{w}^1, \mathbf{z})(\mathbf{u}_K^1)}{\partial \mathbf{u}_K^1} \right|^{-1} \\
& \delta \left(\mathbf{u}_K^2 - \mathbb{G}_{\theta_K}^2 \circ \mathbb{H}_{\theta_K}^1(\mathbf{u}_K^1) \right) \delta \left(\mathbf{u}_K^3 - \mathbb{G}_{\theta_K}^3 \circ \mathbb{H}_{\theta_K}^1(\mathbf{u}_K^1) \right)
\end{aligned} \tag{32}$$

then, by careful inspection of Eq. 31 we can derive the conditional distribution, which is given by:

$$\begin{aligned}
& p(\mathbf{f}_K^1, \mathbf{f}_K^2, \mathbf{f}_K^3 | \mathbf{u}_K^1, \mathbf{u}_K^2, \mathbf{u}_K^3) = \\
& p(\mathbf{f}_0 | \mathbf{u}_0) \prod_{k=0}^{K^1-1} \left| \det \frac{\partial \mathbb{G}_{\theta_k}^1(\mathbf{w}^1, \mathbf{x})(\mathbf{f}_K^1)}{\partial \mathbf{f}_K^1} \right|^{-1} \\
& \delta \left(\mathbf{f}_K^2 - \mathbb{G}_{\theta_K}^2(\mathbf{w}^2, \mathbf{x}) \circ \mathbb{H}_{\theta_K}^1(\mathbf{w}^1, \mathbf{x})(\mathbf{f}_K^1) \right) \delta \left(\mathbf{f}_K^3 - \mathbb{G}_{\theta_K}^3(\mathbf{w}^3, \mathbf{x}) \circ \mathbb{H}_{\theta_K}^1(\mathbf{w}^1, \mathbf{x})(\mathbf{f}_K^1) \right)
\end{aligned} \tag{33}$$

where we have just seen (marked in red in Eq. 31) which elements from the full joint belong to the marginal $p(\mathbf{u}_K^1, \mathbf{u}_K^2, \mathbf{u}_K^3)$, and thus the remaining must belong to the conditional. This gives the prior conditional for C processes:

$$\begin{aligned}
& p(\bar{\mathbf{f}}_K | \bar{\mathbf{u}}_K, \bar{\mathbf{W}}, \mathbf{X}, \mathbf{Z}, \nu) = \underbrace{p(\mathbf{f}_0 | \mathbf{u}_0, \mathbf{X}, \mathbf{Z}, \nu) \prod_{k=0}^{K^1-1} \left| \det \frac{\partial \mathbb{G}_{\theta_k}^1(\mathbf{w}^1, \mathbf{x})(\mathbf{f}_K^1)}{\partial \mathbf{f}_K^1} \right|^{-1}}_{p(\mathbf{f}_K^1 | \mathbf{u}_K^1)} \\
& \prod_{c=2}^C \delta \left(\mathbf{f}_K^c - \mathbb{G}_{\theta_K}^c(\mathbf{w}^c, \mathbf{x}) \circ \mathbb{H}_{\theta_K}^1(\mathbf{w}^1, \mathbf{x})(\mathbf{f}_K^1) \right)
\end{aligned} \tag{34}$$

matching the result in Eq. 30. With this, we are now ready to derive the sparse variational inference algorithm.

A.2.2 Marginal variational distribution $q(\bar{\mathbf{f}}_K)$

The variational distribution is defined following the ideas from [28, 43, 21]:

$$q(\bar{\mathbf{f}}_K, \bar{\mathbf{u}}_K, \bar{\mathbf{W}}) = p(\bar{\mathbf{f}}_K | \bar{\mathbf{u}}_K, \bar{\mathbf{W}}) q(\bar{\mathbf{u}}_K | \bar{\mathbf{W}}) q(\bar{\mathbf{W}}) \tag{35}$$

where we use the conditional model's prior derived in the previous section and a marginal conditional variational distribution that is defined by warping a multivariate Gaussian in the original GP space $q(\mathbf{u}_0 | \mathbf{m}, \mathbf{S})$ using \mathbb{G} , where $\mathbf{m} \in \mathbb{R}^M$, $\mathbf{S} \in \mathbb{R}^{M \times M}$, with the flows from the prior \mathbb{G}_{θ_K} :

$$\begin{aligned}
& q(\bar{\mathbf{u}}_K | \mathbf{m}, \mathbf{S}, \bar{\mathbf{W}}, \mathbf{Z}) = q(\mathbf{u}_0 | \mathbf{m}, \mathbf{S}) \prod_{k=0}^{K^1-1} \left| \det \frac{\partial \mathbb{G}_{\theta_k}^1(\mathbf{w}^1, \mathbf{z})(\mathbf{u}_k^1)}{\partial \mathbf{u}_k^1} \right|^{-1} \\
& \prod_{c=2}^C \delta \left(\mathbf{u}_K^c - \mathbb{G}_{\theta_K}^c(\mathbf{w}^c, \mathbf{z}) \circ \mathbb{H}_{\theta_K}^1(\mathbf{w}^1, \mathbf{z})(\mathbf{u}_K^1) \right)
\end{aligned} \tag{36}$$

and where the distribution over the NN weights factorizes:

$$q(\overline{\mathbf{W}} | \overline{\phi}) = \prod_{c=1}^C q(\mathbf{W}^c | \phi_c) \quad (37)$$

where $\overline{\phi}$ denote variational parameters. Note that the dependence of the marginal $q(\overline{\mathbf{u}}_K)$ on $\overline{\mathbf{W}}$ is required since this distribution is parameterized by the flows of the prior and so inference over $\overline{\mathbf{W}}$ requires dependence between $q(\overline{\mathbf{u}}_K)$ and $q(\overline{\mathbf{W}} | \overline{\phi})$.

To derive our inference algorithm, we need to show how to integrate out inducing points, which turns out that can be done analytically when using diagonal flows, as in [28]:

$$\begin{aligned} q(\overline{\mathbf{f}}_K | \overline{\mathbf{W}}) &= \int_{\mathbf{u}_K^1} \dots \int_{\mathbf{u}_K^C} p(\overline{\mathbf{f}}_K | \overline{\mathbf{u}}_K) q(\overline{\mathbf{u}}_K) d\mathbf{u}_K^1 \dots d\mathbf{u}_K^C \\ &= \int_{\mathbf{u}_K^1} \dots \int_{\mathbf{u}_K^C} p(\mathbf{f}_K^1 | \mathbf{u}_K^1) \prod_{c=2}^C \delta \left(\mathbf{f}_K^c - \mathbb{G}_{\theta_K}^c(\mathbf{w}^c, \mathbf{x}) \circ \mathbb{H}_{\theta_K}^1(\mathbf{w}^1, \mathbf{x})(\mathbf{f}_K^1) \right) \\ &\quad q(\mathbf{u}_K^1) \prod_{c=2}^C \delta \left(\mathbf{u}_K^c - \mathbb{G}_{\theta_K}^c(\mathbf{w}^c, \mathbf{z}) \circ \mathbb{H}_{\theta_K}^1(\mathbf{w}^1, \mathbf{z})(\mathbf{u}_K^1) \right) d\mathbf{u}_K^1 \dots d\mathbf{u}_K^C \\ &= \prod_{c=2}^C \delta \left(\mathbf{f}_K^c - \mathbb{G}_{\theta_K}^c(\mathbf{w}^c, \mathbf{x}) \circ \mathbb{H}_{\theta_K}^1(\mathbf{w}^1, \mathbf{x})(\mathbf{f}_K^1) \right) \\ &\quad \int_{\mathbf{u}_K^1} \dots \int_{\mathbf{u}_K^C} p(\mathbf{f}_K^1 | \mathbf{u}_K^1) q(\mathbf{u}_K^1) \prod_{c=2}^C \delta \left(\mathbf{u}_K^c - \mathbb{G}_{\theta_K}^c(\mathbf{w}^c, \mathbf{z}) \circ \mathbb{H}_{\theta_K}^1(\mathbf{w}^1, \mathbf{z})(\mathbf{u}_K^1) \right) d\mathbf{u}_K^1 \dots d\mathbf{u}_K^C \\ &= \prod_{c=2}^C \delta \left(\mathbf{f}_K^c - \mathbb{G}_{\theta_K}^c(\mathbf{w}^c, \mathbf{x}) \circ \mathbb{H}_{\theta_K}^1(\mathbf{w}^1, \mathbf{x})(\mathbf{f}_K^1) \right) \int_{\mathbf{u}_K^1} p(\mathbf{f}_K^1 | \mathbf{u}_K^1) q(\mathbf{u}_K^1) d\mathbf{u}_K^1 \\ &= \prod_{c=2}^C \delta \left(\mathbf{f}_K^c - \mathbb{G}_{\theta_K}^c(\mathbf{w}^c, \mathbf{x}) \circ \mathbb{H}_{\theta_K}^1(\mathbf{w}^1, \mathbf{x})(\mathbf{f}_K^1) \right) \prod_{k=0}^{K^1-1} \left| \det \frac{\partial \mathbb{G}_{\theta_k}^1(\mathbf{w}^1, \mathbf{x})(\mathbf{f}_K^1)}{\partial \mathbf{f}_K^1} \right|^{-1} \\ &\quad \int p(\mathbf{f}_0 | \mathbf{u}_0) q(\mathbf{u}_0) d\mathbf{u}_0 \\ &= q(\mathbf{f}_0) \prod_{k=0}^{K^1-1} \left| \det \frac{\partial \mathbb{G}_{\theta_k}^1(\mathbf{w}^1, \mathbf{x})(\mathbf{f}_K^1)}{\partial \mathbf{f}_K^1} \right|^{-1} \prod_{c=2}^C \delta \left(\mathbf{f}_K^c - \mathbb{G}_{\theta_K}^c(\mathbf{w}^c, \mathbf{x}) \circ \mathbb{H}_{\theta_K}^1(\mathbf{w}^1, \mathbf{x})(\mathbf{f}_K^1) \right) \end{aligned} \quad (38)$$

where $q(\mathbf{f}_0)$ is given by Eq. 21. Note that the form of this marginal variational distribution $q(\overline{\mathbf{f}}_K)$ implies the following generative procedure already used in the definition of the ETGP:

$$\begin{aligned} \mathbf{f}_0 &\sim q(\mathbf{f}_0) \\ \mathbf{f}_K^1 &= \mathbb{G}_{\theta_K}^1(\mathbf{w}^1, \mathbf{x})(\mathbf{f}_0), \quad \mathbf{f}_K^2 = \mathbb{G}_{\theta_K}^2(\mathbf{w}^2, \mathbf{x})(\mathbf{f}_0) \quad \dots \quad \mathbf{f}_K^C = \mathbb{G}_{\theta_K}^C(\mathbf{w}^C, \mathbf{x})(\mathbf{f}_0) \end{aligned} \quad (39)$$

The sequence of steps used in the derivation are the followings. We start by writing the marginalization in terms of the conditional distribution $p(\overline{\mathbf{f}}_K | \overline{\mathbf{u}}_K, \overline{\mathbf{W}})$ and the proposed marginal variational $q(\overline{\mathbf{u}}_K | \overline{\mathbf{W}})$. From second to third equality we take out from the integral the terms that do not depend on $\overline{\mathbf{u}}_K$. Then from third to fourth equality we integrate out all $\overline{\mathbf{u}}_K$ except the *pivot* \mathbf{u}_K^1 . Note that integration here is straightforward since the Dirac measure integrates to 1². This let us with one integral over \mathbf{u}_K^1 . From fourth to fifth equality, we write $p(\mathbf{f}_K^1 | \mathbf{u}_K^1)$ using the expression in Eq. 34, and since the Jacobian does not depend on \mathbf{u}_K^1 it is taken out from the integral. Lastly, we apply the LOTUS rule (see appendix in [28] and below) by noting an expectation over $q(\mathbf{u}_K^1)$, which give us a simple Gaussian integral, from which analytical solution $q(\mathbf{f}_0)$ is well known. This distribution coincides with the SVGP marginal variational given by Eq. 21, as in TGPs.

For self-contained purposes we copy the LOTUS rule definition in [28]:

²Readers concerned with the integration of the Dirac measure in this context can replace it by a Gaussian density taking the limit of $\sigma \rightarrow 0$.

LOTUS rule: Given an invertible transformation \mathbb{G} , and the distribution $p(\mathbf{f}_K)$ induced by transforming samples from a base distribution $p(\mathbf{f}_0)$, then it holds that expectations of any function $h(\cdot)$ under $p(\mathbf{f}_K)$ can be computed by integrating w.r.t. the base distribution $p(\mathbf{f}_0)$. This is formally known as probability under change of measure. Formally, the above statement implies:

$$\mathbb{E}_{p(\mathbf{f}_K)} [h(\mathbf{f}_K)] = \mathbb{E}_{p(\mathbf{f}_0)} [h(\mathbb{G}(\mathbf{f}_0))] \quad (40)$$

A.2.3 Evidence Lower Bound ELBO

The Evidence Lower Bound resulting from the prior model and the variational approximate posterior can be written down as:

$$\begin{aligned} \text{ELBO} &= \int_{\bar{\mathbf{f}}_K} \int_{\bar{\mathbf{u}}_K} \int_{\bar{\mathbf{W}}} q(\bar{\mathbf{f}}_K, \bar{\mathbf{u}}_K | \bar{\mathbf{W}}) q(\bar{\mathbf{W}}) \frac{\log p(\mathbf{y} | \bar{\mathbf{f}}_K) p(\bar{\mathbf{f}}_K, \bar{\mathbf{u}}_K | \bar{\mathbf{W}}) p(\bar{\mathbf{W}})}{q(\bar{\mathbf{f}}_K, \bar{\mathbf{u}}_K | \bar{\mathbf{W}}) q(\bar{\mathbf{W}})} d\bar{\mathbf{f}}_K d\bar{\mathbf{u}}_K d\bar{\mathbf{W}} \\ &= \underbrace{\int_{\bar{\mathbf{f}}_K} \int_{\bar{\mathbf{u}}_K} \int_{\bar{\mathbf{W}}} q(\bar{\mathbf{f}}_K, \bar{\mathbf{u}}_K | \bar{\mathbf{W}}) q(\bar{\mathbf{W}}) \log p(\mathbf{y} | \bar{\mathbf{f}}_K) d\bar{\mathbf{f}}_K d\bar{\mathbf{u}}_K d\bar{\mathbf{W}}}_{\text{ELL}} \\ &\quad + \underbrace{\int_{\bar{\mathbf{f}}_K} \int_{\bar{\mathbf{u}}_K} \int_{\bar{\mathbf{W}}} q(\bar{\mathbf{f}}_K, \bar{\mathbf{u}}_K | \bar{\mathbf{W}}) q(\bar{\mathbf{W}}) \log \frac{p(\bar{\mathbf{f}}_K, \bar{\mathbf{u}}_K | \bar{\mathbf{W}}) p(\bar{\mathbf{W}})}{q(\bar{\mathbf{f}}_K, \bar{\mathbf{u}}_K | \bar{\mathbf{W}}) q(\bar{\mathbf{W}})} d\bar{\mathbf{f}}_K d\bar{\mathbf{u}}_K d\bar{\mathbf{W}}}_{-\text{KLD}} \end{aligned} \quad (41)$$

where we again drop the conditioning set, except $\bar{\mathbf{W}}$, for clarity. Working each term separately yields:

$$\begin{aligned} -\text{KLD} &= \int_{\bar{\mathbf{f}}_K} \int_{\bar{\mathbf{u}}_K} \int_{\bar{\mathbf{W}}} q(\bar{\mathbf{f}}_K, \bar{\mathbf{u}}_K | \bar{\mathbf{W}}) q(\bar{\mathbf{W}}) \log \frac{p(\bar{\mathbf{f}}_K, \bar{\mathbf{u}}_K | \bar{\mathbf{W}}) p(\bar{\mathbf{W}})}{q(\bar{\mathbf{f}}_K, \bar{\mathbf{u}}_K | \bar{\mathbf{W}}) q(\bar{\mathbf{W}})} d\bar{\mathbf{f}}_K d\bar{\mathbf{u}}_K d\bar{\mathbf{W}} \\ &= \int_{\bar{\mathbf{f}}_K} \int_{\bar{\mathbf{u}}_K} \int_{\bar{\mathbf{W}}} q(\bar{\mathbf{f}}_K, \bar{\mathbf{u}}_K | \bar{\mathbf{W}}) q(\bar{\mathbf{W}}) \log \frac{p(\bar{\mathbf{f}}_K | \bar{\mathbf{u}}_K, \bar{\mathbf{W}}) p(\bar{\mathbf{u}}_K | \bar{\mathbf{W}}) p(\bar{\mathbf{W}})}{p(\bar{\mathbf{f}}_K | \bar{\mathbf{u}}_K, \bar{\mathbf{W}}) q(\bar{\mathbf{u}}_K | \bar{\mathbf{W}}) q(\bar{\mathbf{W}})} d\bar{\mathbf{f}}_K d\bar{\mathbf{u}}_K d\bar{\mathbf{W}} \\ &= \int_{\bar{\mathbf{f}}_K} \int_{\bar{\mathbf{u}}_K} \int_{\bar{\mathbf{W}}} q(\bar{\mathbf{f}}_K, \bar{\mathbf{u}}_K | \bar{\mathbf{W}}) q(\bar{\mathbf{W}}) \log \frac{\prod_{c=2}^C \delta(\mathbf{u}_K^c - \mathbb{G}_{\theta_K^c}^c(\mathbf{w}^c, \mathbf{z}) \circ \mathbb{H}_{\theta_K^1}^1(\mathbf{w}^1, \mathbf{z})(\mathbf{u}_K^1))}{\prod_{c=2}^C \delta(\mathbf{u}_K^c - \mathbb{G}_{\theta_K^c}^c(\mathbf{w}^c, \mathbf{z}) \circ \mathbb{H}_{\theta_K^1}^1(\mathbf{w}^1, \mathbf{z})(\mathbf{u}_K^1))} d\bar{\mathbf{f}}_K d\bar{\mathbf{u}}_K d\bar{\mathbf{W}} \\ &\quad + \int_{\bar{\mathbf{f}}_K} \int_{\bar{\mathbf{u}}_K} \int_{\bar{\mathbf{W}}} q(\bar{\mathbf{f}}_K, \bar{\mathbf{u}}_K | \bar{\mathbf{W}}) q(\bar{\mathbf{W}}) \log \frac{p(\mathbf{u}_K^1 | \mathbf{W}^1) p(\bar{\mathbf{W}})}{q(\mathbf{u}_K^1 | \mathbf{W}^1) q(\bar{\mathbf{W}})} d\bar{\mathbf{f}}_K d\bar{\mathbf{u}}_K d\bar{\mathbf{W}} \\ &= \int_{\bar{\mathbf{u}}_K} \int_{\bar{\mathbf{W}}} q(\mathbf{u}_K^1 | \mathbf{W}^1) \prod_{c=2}^C \delta(\mathbf{u}_K^c - \mathbb{G}_{\theta_K^c}^c(\mathbf{w}^c, \mathbf{z}) \circ \mathbb{H}_{\theta_K^1}^1(\mathbf{w}^1, \mathbf{z})(\mathbf{u}_K^1)) q(\bar{\mathbf{W}}) \log \frac{p(\mathbf{u}_K^1 | \mathbf{W}^1) p(\bar{\mathbf{W}})}{q(\mathbf{u}_K^1 | \mathbf{W}^1) q(\bar{\mathbf{W}})} d\bar{\mathbf{u}}_K d\bar{\mathbf{W}} \\ &= \int_{\bar{\mathbf{u}}_K^1} \int_{\bar{\mathbf{W}}} q(\mathbf{u}_K^1 | \mathbf{W}^1) q(\bar{\mathbf{W}}) \log \frac{p(\mathbf{u}_K^1 | \mathbf{W}^1) p(\bar{\mathbf{W}})}{q(\mathbf{u}_K^1 | \mathbf{W}^1) q(\bar{\mathbf{W}})} d\mathbf{u}_K^1 d\bar{\mathbf{W}} \\ &= \int_{\bar{\mathbf{W}}} q(\bar{\mathbf{W}}) \int_{\mathbf{u}_K^1} q(\mathbf{u}_K^1 | \mathbf{W}^1) \log \frac{p(\mathbf{u}_K^1 | \mathbf{W}^1)}{q(\mathbf{u}_K^1 | \mathbf{W}^1)} d\mathbf{u}_K^1 d\bar{\mathbf{W}} + \int_{\bar{\mathbf{W}}} q(\bar{\mathbf{W}}) \log \frac{p(\bar{\mathbf{W}})}{q(\bar{\mathbf{W}})} d\bar{\mathbf{W}} \\ &= \int_{\bar{\mathbf{W}}} q(\bar{\mathbf{W}}) \int_{\mathbf{u}_0} q(\mathbf{u}_0) \log \frac{p(\mathbf{u}_0)}{q(\mathbf{u}_0)} d\mathbf{u}_0 d\bar{\mathbf{W}} + \int_{\bar{\mathbf{W}}} q(\bar{\mathbf{W}}) \log \frac{p(\bar{\mathbf{W}})}{q(\bar{\mathbf{W}})} d\bar{\mathbf{W}} \\ &= -\text{KLD}[q(\mathbf{u}_0) || p(\mathbf{u}_0)] - \text{KLD}[q(\bar{\mathbf{W}}) || p(\bar{\mathbf{W}})] \end{aligned} \quad (42)$$

where in the second and third equalities we cancel common terms. From equality 3 to 4 we integrate out all $\bar{\mathbf{f}}_K$ since nothing depends on them. In step from equality 4 to 5 we integrate out the Dirac measures over all the non-*pivot* elements. From equality 5 to 6 we separate expectations and step 6 to 7 can be derived in two ways. First, since KLD is invariant under a parameter transformation (reparameterization) and both the prior and variational distributions are transformed with the same warping function $\bar{\mathbb{G}}_{\theta_K}$, then the KLD can be written as that on the original GP space. Another way to

derive this KLD is by noting an expected value of a log-ratio w.r.t. $q(\bar{\mathbf{u}}_K)$, allowing us to apply the LOTUS rule, and corresponding Jacobian cancellations. More precisely:

$$\begin{aligned}
& \int_{\mathbf{u}_K^1} q(\mathbf{u}_K^1) \log \frac{p(\mathbf{u}_K^1)}{q(\mathbf{u}_K^1)} d\mathbf{u}_K^1 \\
&= \int_{\mathbf{u}_K^1} q(\mathbf{u}_K^1) \log \frac{p(\mathbf{u}_0 | \mathbf{z}, \nu) \prod_{k=0}^{K^1-1} \left| \det \frac{\partial \mathbb{G}_{\theta_k^1(\mathbf{w}^1, \mathbf{z})}(\mathbf{u}_k^1)}{\partial \mathbf{u}_k^1} \right|^{-1}}{q(\mathbf{u}_0 | \mathbf{m}, \mathbf{S}) \prod_{k=0}^{K^1-1} \left| \det \frac{\partial \mathbb{G}_{\theta_k^1(\mathbf{w}^1, \mathbf{z})}(\mathbf{u}_k^1)}{\partial \mathbf{u}_k^1} \right|^{-1}} d\mathbf{u}_K^1 \\
&= \int_{\mathbf{u}_0} q(\mathbf{u}_0) \log \frac{p(\mathbf{u}_0 | \mathbf{z}, \nu)}{q(\mathbf{u}_0 | \mathbf{m}, \mathbf{S})} d\mathbf{u}_0
\end{aligned} \tag{43}$$

which is a similar derivation to that in [28]. Note that we could also recognize the LOTUS rule being applied from equality 3 to equality 7 directly in Eq. 42, by previously integrating out $\bar{\mathbf{f}}_K$ and without the $\delta(\cdot)$ cancellations. In other words, we can see the full KLD over $\bar{\mathbf{u}}_K$ as a direct reparameterization applied to \mathbf{u}_0 .

We next derive the ELL:

$$\begin{aligned}
\text{ELL} &= \int_{\bar{\mathbf{W}}} \int_{\bar{\mathbf{f}}_K} \int_{\bar{\mathbf{u}}_K} q(\bar{\mathbf{f}}_K, \bar{\mathbf{u}}_K | \bar{\mathbf{W}}) q(\bar{\mathbf{W}}) \log p(\mathbf{y} | \bar{\mathbf{f}}_K) d\bar{\mathbf{f}}_K d\bar{\mathbf{u}}_K d\bar{\mathbf{W}} \\
&= \int_{\bar{\mathbf{W}}} \int_{\bar{\mathbf{f}}_K} q(\bar{\mathbf{f}}_K | \bar{\mathbf{W}}) q(\bar{\mathbf{W}}) \log p(\mathbf{y} | \bar{\mathbf{f}}_K) d\bar{\mathbf{f}}_K d\bar{\mathbf{W}} \\
&= \int_{\bar{\mathbf{W}}} \int_{\mathbf{f}_0} q(\mathbf{f}_0) q(\bar{\mathbf{W}}) \log p(\mathbf{y} | \bar{\mathbb{G}}_{\theta_K(\bar{\mathbf{w}}, \mathbf{x})}(\mathbf{f}_0)) d\mathbf{f}_0 d\bar{\mathbf{W}} \\
&= \int_{\bar{\mathbf{W}}} \int_{\mathbf{f}_0} q(\mathbf{f}_0) q(\bar{\mathbf{W}}) \log \prod_{n=1}^N \prod_{c=1}^C \pi_c(\bar{\mathbb{G}}_{\theta_K(\bar{\mathbf{w}}, \mathbf{x}^n)}(f_{0,n}))^{\mathbb{I}(y^n=c)} d\mathbf{f}_0 d\bar{\mathbf{W}} \\
&= \sum_{n=1}^N \sum_{c=1}^C \mathbb{I}(y^n=c) \int_{\bar{\mathbf{W}}} q(\bar{\mathbf{W}}) \int_{f_{0,n}} q(f_{0,n}) \log \pi_c(\bar{\mathbb{G}}_{\theta_K(\bar{\mathbf{w}}, \mathbf{x}^n)}(f_{0,n})) df_{0,n} d\bar{\mathbf{W}} \\
&\approx \sum_{n=1}^N \sum_{c=1}^C \mathbb{I}(y^n=c) \frac{1}{S} \sum_{s=1}^S \int_{f_{0,n}} q(f_{0,n}) \log \pi_c(\bar{\mathbb{G}}_{\theta_K(\bar{\mathbf{w}}^s, \mathbf{x}^n)}(f_{0,n})) df_{0,n}; \bar{\mathbf{W}}_s \sim q(\bar{\mathbf{W}})
\end{aligned} \tag{44}$$

where we first integrate out $\bar{\mathbf{u}}_K$ yielding the derived conditional marginal $q(\bar{\mathbf{f}}_K | \bar{\mathbf{W}})$ and then apply the LOTUS rule to expectation w.r.t. $q(\bar{\mathbf{f}}_K | \bar{\mathbf{W}})$. The remaining steps are similar to SVGP when plugging the specific Categorical Likelihood used in this work.

Using both derivations we recover the ELBO in the main paper (Eq. 10):

$$\begin{aligned}
\text{ELBO} &= \sum_{n=1}^N \sum_{c=1}^C \mathbb{I}(y^n=c) \int_{\bar{\mathbf{W}}} q(\bar{\mathbf{W}}) \int_{f_{0,n}} q(f_{0,n}) \log \pi_c(\bar{\mathbb{G}}_{\theta_K(\bar{\mathbf{w}}, \mathbf{x}^n)}(f_{0,n})) df_{0,n} d\bar{\mathbf{W}} \\
&\quad - \text{KLD}[q(\mathbf{u}_0) || p(\mathbf{u}_0)] - \text{KLD}[q(\bar{\mathbf{W}}) || p(\bar{\mathbf{W}})]
\end{aligned} \tag{45}$$

A.2.4 Computational advantages

We highlight differences between our proposed model and SVGPs. First, expectations w.r.t. $q(\mathbf{f}_0)$ in Eq. 45 can be computed with 1-d quadrature. By contrast, the SVGP method cannot use quadrature methods and require Monte Carlo. This makes our algorithm computationally advantageous. On the other side expectations w.r.t. the NN's parameters can be computed using batched matrix multiplications and in practice we use Monte Carlo Dropout [15] with one Monte Carlo sample for training, making this computation very efficient. Moreover, the number of GP operations is constant with C . To get $q(\mathbf{f}^c)$ in SVGPs one needs a cubic operation to invert $K_\nu^c(\mathbf{Z}, \mathbf{Z})$ and M^2 operation to compute the variational parameters per class and datapoint, giving a complexity of $\mathcal{O}(CM^3 + CNM^2)$. This can be alleviated by sharing K_ν and \mathbf{Z} across GPs, resulting in

$\mathcal{O}(M^3 + CNM^2)$, at the cost of limiting expressiveness, as shown in the experiment section. ETGP cost is always $\mathcal{O}(M^3 + NM^2)$ (without considering the NN's computations, which for the architecture presented is often much faster and can be done in parallel to GP operations).

A.3 Proof of proposition 1

In this section we prove proposition 1, which we restate for clarity.

Proposition 1. *The joint conditional distribution of C non-stationary GPs obtained via a linear flow is given by:*

$$p(\bar{\mathbf{f}}_K | \bar{\mathbf{W}}) = \mathcal{N}(\mathbf{f}_K^1 | \mathbf{b}^1, \mathbf{A}_1 K_\nu(\mathbf{X}, \mathbf{X}) \mathbf{A}_1^T) \prod_{c=2}^C \delta\left(\mathbf{f}_K^c - \mathbb{G}_{\theta_K^c}^c(\mathbf{w}^c, \mathbf{X}) \circ \mathbb{H}_{\theta_K^c}^1(\mathbf{w}^1, \mathbf{X})(\mathbf{f}_K^1)\right), \quad (46)$$

with $\mathbf{b}^1 = (b^1(\mathbf{x}^1), \dots, b^1(\mathbf{x}^N))^T$ and $\mathbf{A}_1 \in \mathbb{R}^{N \times N}$ a diagonal matrix with entries $\mathbf{a}^1 = (a^1(\mathbf{x}^1), \dots, a^1(\mathbf{x}^N))^T$. Each marginal $p(\mathbf{f}_K^c)$ is Gaussian with mean and covariance given by \mathbf{b}^c and $\mathbf{A}_c K_\nu(\mathbf{X}, \mathbf{X}) \mathbf{A}_c^T$, respectively. The covariance matrix between the pivot \mathbf{f}_K^1 and \mathbf{f}_K^c , for $c \neq 1$, is given by: $\mathbf{a}^1 (\mathbf{a}^c)^T \odot K_\nu(\mathbf{X}, \mathbf{X})$ with \odot denoting Hadamart product.

The proof is divided in two steps. We first derive the marginal distributions $\{p(\mathbf{f}_K^c)\}_{c=1}^C$ and then the covariances. For all the proof we will assume that the pivot is \mathbf{f}_K^1 . First, since a linear flow is used, we can write the flow mapping over a set of samples $\mathbf{X} = (\mathbf{x}^1, \dots, \mathbf{x}^N)$ in matrix form as:

$$\mathbf{f}_K^1 = \mathbf{A}_1 \mathbf{f}_0 + \mathbf{b}^1 \quad (47)$$

with $\mathbf{A}_1 \in \mathbb{R}^{N \times N}$ being a diagonal matrix with entries $\mathbf{a}^1 = (a^1(\mathbf{x}^1), \dots, a^1(\mathbf{x}^N))^T$ and $\mathbf{b}^1 = (b^1(\mathbf{x}^1), \dots, b^1(\mathbf{x}^N))^T$. Thus, using the fact that $p(\mathbf{f}_0 | \mathbf{X}, \nu) = \mathcal{N}(\mathbf{f}_0 | \mathbf{0}, K_\nu(\mathbf{X}, \mathbf{X}))$ and the resulting density when applying a linear transformation to a Gaussian density, the marginal distribution over \mathbf{f}_K^1 is:

$$\mathcal{N}(\mathbf{f}_K^1 | \mathbf{b}^1, \mathbf{A}_1 K_\nu(\mathbf{X}, \mathbf{X}) \mathbf{A}_1^T) \quad (48)$$

Note that for non-zero mean GP the mean would be given by $\mathbf{b}^1 + \mathbf{A}_1 \mu_\nu(\mathbf{X})$. To derive the marginal distribution for each c we solve the following integral:

$$\begin{aligned} p(\mathbf{f}_K^c) &= \int_{\mathbf{f}_K^1} p(\mathbf{f}_K^1) p(\mathbf{f}_K^c | \mathbf{f}_K^1) d\mathbf{f}_K^1 \\ &= \int_{\mathbf{f}_K^1} \mathcal{N}(\mathbf{f}_K^1 | \mathbf{b}^1, \mathbf{A}_1 K_\nu(\mathbf{X}, \mathbf{X}) \mathbf{A}_1^T) \delta\left(\mathbf{f}_K^c - \mathbb{G}_{\theta_K^c}^c(\mathbf{w}^c, \mathbf{X}) \circ \mathbb{H}_{\theta_K^c}^1(\mathbf{w}^1, \mathbf{X})(\mathbf{f}_K^1)\right) d\mathbf{f}_K^1 \end{aligned} \quad (49)$$

Before solving it note that for any c we have:

$$\begin{aligned} \mathbf{f}_K^c &= \mathbb{G}_{\theta_K^c}^c(\mathbf{w}^c, \mathbf{X}) \circ \mathbb{H}_{\theta_K^c}^1(\mathbf{w}^1, \mathbf{X})(\mathbf{f}_K^1) \\ &= \underbrace{\mathbf{A}_c \mathbf{A}_1^{-1} [\mathbf{f}_K^1 - \mathbf{b}^1]}_{\mathbb{H}} + \mathbf{b}^c \end{aligned} \quad (50)$$

yielding:

$$\begin{aligned} p(\mathbf{f}_K^c) &= \int_{\mathbf{f}_K^1} \mathcal{N}(\mathbf{f}_K^1 | \mathbf{b}^1, \mathbf{A}_1 K_\nu(\mathbf{X}, \mathbf{X}) \mathbf{A}_1^T) \delta(\mathbf{f}_K^c - \mathbf{A}_c \mathbf{A}_1^{-1} [\mathbf{f}_K^1 - \mathbf{b}^1] - \mathbf{b}^c) d\mathbf{f}_K^1 \\ &= \int_{\mathbf{f}_K^1} \mathcal{N}(\mathbf{f}_K^1 | \mathbf{b}^1, \mathbf{A}_1 K_\nu(\mathbf{X}, \mathbf{X}) \mathbf{A}_1^T) \delta(\mathbf{f}_K^c - \mathbf{A}_c \mathbf{A}_1^{-1} \mathbf{f}_K^1 + \mathbf{A}_c \mathbf{A}_1^{-1} \mathbf{b}^1 - \mathbf{b}^c) d\mathbf{f}_K^1 \end{aligned} \quad (51)$$

We then rewrite this last expression to highlight the integral to be solved:

$$\int_{\mathbf{f}_K^1} \mathcal{N}(\mathbf{f}_K^1 | \mathbf{m}, \mathbf{S}) \delta(\mathbf{f}_K^c - \mathbf{Q} \mathbf{f}_K^1 - \mathbf{r}) d\mathbf{f}_K^1 \quad (52)$$

with:

$$\begin{aligned}
\mathbf{m} &= \mathbf{b}^1 \\
\mathbf{S} &= \mathbf{A}_1 K_\nu(\mathbf{X}, \mathbf{X}) \mathbf{A}_1^\top \\
\mathbf{Q} &= \mathbf{A}_c \mathbf{A}_1^{-1} \\
\mathbf{r} &= -\mathbf{A}_c \mathbf{A}_1^{-1} \mathbf{b}^1 + \mathbf{b}^c
\end{aligned} \tag{53}$$

The solution of this integral is obtained by the following procedure. First note that if $\mathbf{Q} = \mathbf{I}$ we recognize a convolution between a Gaussian and a Dirac delta function, easily solved by applying the selection property of Dirac delta functions:

$$\begin{aligned}
\mathcal{N}(\mathbf{f}_K^c | \mathbf{m}, \mathbf{S}) \otimes \delta(\mathbf{f}_K^c - \mathbf{r}) &:= \int_{-\infty}^{\infty} \mathcal{N}(\mathbf{f}_K^1 | \mathbf{m}, \mathbf{S}) \delta(\mathbf{f}_K^c - \mathbf{f}_K^1 - \mathbf{r}) d\mathbf{f}_K^1 \\
&= \mathcal{N}(\mathbf{f}_K^c - \mathbf{r} | \mathbf{m}, \mathbf{S}) = \mathcal{N}(\mathbf{f}_K^c | \mathbf{m} + \mathbf{r}, \mathbf{S})
\end{aligned} \tag{54}$$

where the last step holds by writing the Gaussian density and checking $\mathbf{f}_K^c - \mathbf{r} - \mathbf{m} = \mathbf{f}_K^c - (\mathbf{m} + \mathbf{r})$. For $\mathbf{Q} \neq \mathbf{I}$, we perform an integration by substitution³, since there is no way we can write the integral as a convolution between two functions. More precisely let $u = \mathbf{Q}\mathbf{f}_K^1 + \mathbf{r}$. We have $\mathbf{f}_K^1 = \mathbf{Q}^{-1}(u - \mathbf{r})$ and $|\det du/d\mathbf{f}_K^1| = |\det \mathbf{Q}|$ which implies the substitution $d\mathbf{f}_K^1 = |1/\det \mathbf{Q}| du$. Putting all together we have:

$$\begin{aligned}
p(\mathbf{f}_K^c) &= \int_{\mathbf{f}_K^1} \mathcal{N}(\mathbf{f}_K^1 | \mathbf{m}, \mathbf{S}) \delta(\mathbf{f}_K^c - \mathbf{Q}\mathbf{f}_K^1 - \mathbf{r}) d\mathbf{f}_K^1 \\
&= \int_{\mathbf{f}_K^1} \mathcal{N}(\mathbf{Q}^{-1}(u - \mathbf{r}) | \mathbf{m}, \mathbf{S}) \delta(\mathbf{f}_K^c - u) \left| \frac{1}{\det \mathbf{Q}} \right| du \\
&= \frac{1}{|\det \mathbf{Q}|} \mathcal{N}(\mathbf{Q}^{-1}(\mathbf{f}_K^c - \mathbf{r}) | \mathbf{m}, \mathbf{S})
\end{aligned} \tag{55}$$

Beyond the substitution the integral is solved by applying the selection property of the delta function. After applying some standard algebra to the Gaussian distribution (see App. A.5) we have:

$$\mathcal{N}(\mathbf{Q}^{-1}(\mathbf{f}_K^c - \mathbf{r}) | \mathbf{m}, \mathbf{S}) = |\det \mathbf{Q}| \mathcal{N}(\mathbf{f}_K^c | \mathbf{Q}\mathbf{m} + \mathbf{r}, \mathbf{Q}\mathbf{S}\mathbf{Q}^\top) \tag{56}$$

Giving the final result:

$$p(\mathbf{f}_K^c) = \mathcal{N}(\mathbf{f}_K^c | \mathbf{Q}\mathbf{m} + \mathbf{r}, \mathbf{Q}\mathbf{S}\mathbf{Q}^\top) \tag{57}$$

since $|\det \mathbf{Q}|$ cancels with $1/|\det \mathbf{Q}|$. Note this result matches the one obtained with the convolution for $\mathbf{Q} = \mathbf{I}$. If we now substitute the shortcuts for $\mathbf{Q}, \mathbf{S}, \mathbf{m}, \mathbf{r}$ we have for the covariance:

$$\begin{aligned}
\mathbf{Q}\mathbf{S}\mathbf{Q}^\top &= \mathbf{A}_c \mathbf{A}_1^{-1} \mathbf{A}_1 K_\nu(\mathbf{X}, \mathbf{X}) \mathbf{A}_1^\top [\mathbf{A}_c \mathbf{A}_1^{-1}]^\top \\
&= \mathbf{A}_c \mathbf{A}_1^{-1} \mathbf{A}_1 K_\nu(\mathbf{X}, \mathbf{X}) \mathbf{A}_1 \mathbf{A}_1^{-1} \mathbf{A}_c \\
&= \mathbf{A}_c K_\nu(\mathbf{X}, \mathbf{X}) \mathbf{A}_c
\end{aligned} \tag{58}$$

where we apply some standard matrix identities. In particular the transpose of the product is the product of the transposes in reverse order, and the transpose of a diagonal matrix is equal to the diagonal matrix. For the mean we have:

$$\mathbf{r} + \mathbf{Q}\mathbf{m} = \cancel{-\mathbf{A}_c \mathbf{A}_1^{-1} \mathbf{b}^1} + \mathbf{b}^c + \cancel{\mathbf{A}_c \mathbf{A}_1^{-1} \mathbf{b}^1} = \mathbf{b}^c \tag{59}$$

finishing the first part of the proof, which we re-emphasize:

The marginal distribution for any \mathbf{f}_K^c has density given by: $\mathcal{N}(\mathbf{f}_K^c | \mathbf{b}^c, \mathbf{A}_c K_\nu(\mathbf{X}, \mathbf{X}) \mathbf{A}_c^\top)$

Importantly, note that if non-zero GPs are used, this result is also matched with the particularity that the mean is given by $\mathbf{b}^c + \mathbf{A}_c \mu_\nu(\mathbf{X})$. This is seen by replacing $\mathbf{A}_c \mathbf{A}_1^{-1} \mathbf{b}^1$ for $\mathbf{A}_c \mathbf{A}_1^{-1} [\mathbf{b}^1 + \mathbf{A}_1 \mu_\nu(\mathbf{X})]$ in Eq. 59.

The second part of the proof characterizes some of the linear dependencies (covariance) in the joint distribution $p(\bar{\mathbf{f}}_K)$. We note that in this paper we have not figured out the form of the joint distribution if the *pivot* is integrated out, i.e. how the pivot couples the rest of latent functions. In other words,

³After this derivation we found a simpler way to obtain this solution which is given, for completeness, in App. A.4.

the distribution $p(\mathbf{f}_K^2, \dots, \mathbf{f}_K^C) = \int_{\mathbf{f}_K^1} p(\mathbf{f}_K^2, \dots, \mathbf{f}_K^C | \mathbf{f}_K^1) p(\mathbf{f}_K^1) d\mathbf{f}_K^1$ is unknown, which limits the full characterization of the covariances in the joint distribution.

For this reason in this proposition we just characterize the covariances between any \mathbf{f}_K^c and the *pivot* \mathbf{f}_K^1 . For this we use the expression:

$$\text{COV}[\mathbf{f}_K^1, \mathbf{f}_K^c] = \mathbb{E}[\mathbf{f}_K^1 (\mathbf{f}_K^c)^\top] - \mathbb{E}[\mathbf{f}_K^1] \mathbb{E}[\mathbf{f}_K^c]^\top \quad (60)$$

The expected values can be directly obtained from the marginal distributions obtained in the first part of the proof. In particular:

$$\begin{aligned} \mathbb{E}[\mathbf{f}_K^1] &= \mathbf{b}^1 \\ \mathbb{E}[\mathbf{f}_K^c] &= \mathbf{b}^c \end{aligned} \quad (61)$$

To derive the covariance, it is easier to do it by just looking at its entries at two single points locations \mathbf{x}^n and $\mathbf{x}^{n'}$ and then generalizing the result. Following the main paper notation we have $f_{0,n} := f_0(\mathbf{x}^n)$, $b^c(\mathbf{x}^n) := b_n^c$ and $a^c(\mathbf{x}^n) := a_n^c$.

A.3.1 Covariance between $f_{K,n}^1$ and $f_{K,n}^c$ at a single location n

For this we compute:

$$\begin{aligned} \mathbb{E}[f_{K,n}^1 f_{K,n}^c] &= \int_{f_{K,n}^1} \int_{f_{K,n}^c} f_{K,n}^1 f_{K,n}^c \mathcal{N}(f_{K,n}^1 | b_n^1, a_n^1 K_\nu(\mathbf{x}^n, \mathbf{x}^n) a_n^1) \delta\left(f_{K,n}^c - \frac{a_n^c}{a_n^1} [f_{K,n}^1 - b_n^1] - b_n^c\right) df_{K,n}^1 df_{K,n}^c \\ &= \int_{f_{K,n}^1} \left[\frac{a_n^c}{a_n^1} f_{K,n}^1 f_{K,n}^1 - \frac{a_n^c}{a_n^1} b_n^1 f_{K,n}^1 + b_n^c f_{K,n}^1 \right] \mathcal{N}(f_{K,n}^1 | b_n^1, a_n^1 K_\nu(\mathbf{x}^n, \mathbf{x}^n) a_n^1) df_{K,n}^1 \\ &= \frac{a_n^c}{a_n^1} \left[a_n^1 K_\nu(\mathbf{x}^n, \mathbf{x}^n) a_n^1 + (b_n^1)^2 \right] - \frac{a_n^c}{a_n^1} (b_n^1)^2 + b_n^c b_n^1 \\ &= a_n^c K_\nu(\mathbf{x}^n, \mathbf{x}^n) a_n^1 + b_n^c b_n^1 \end{aligned} \quad (62)$$

yielding,

$$\begin{aligned} \text{COV}[f_{K,n}^1, f_{K,n}^c] &= \mathbb{E}[f_{K,n}^1 f_{K,n}^c] - \mathbb{E}[f_{K,n}^1] \mathbb{E}[f_{K,n}^c] \\ &= a_n^c K_\nu(\mathbf{x}^n, \mathbf{x}^n) a_n^1 + b_n^c b_n^1 - b_n^c b_n^1 \\ &= a_n^c K_\nu(\mathbf{x}^n, \mathbf{x}^n) a_n^1 \end{aligned} \quad (63)$$

So the covariance between two processes at all locations N will be given by the diagonal of $K_\nu(\mathbf{X}, \mathbf{X})$ element-wise multiplied by the diagonal of $\mathbf{a}^1 (\mathbf{a}^c)^\top$.

A.3.2 Covariance between $f_{K,n}^1$ and $f_{K,n'}^c$ at different locations n, n'

We again emphasize the main paper notation for easier presentation and re-highlight that for this particular section $\mathbf{f}_K^1 = (f_{K,n}^1, f_{K,n'}^1)^\top$ and similar for any parameter short cut e.g. \mathbf{b}^1 . For this we compute:

$$\begin{aligned} \mathbb{E}[f_{K,n}^1 f_{K,n'}^c] &= \int_{f_{K,n}^1} \int_{f_{K,n'}^1} \int_{f_{K,n'}^c} f_{K,n}^1 f_{K,n'}^c \mathcal{N}(\mathbf{f}_K^1 | \mathbf{b}^1, \mathbf{A}_1 K_\nu(\mathbf{X}, \mathbf{X}) \mathbf{A}_1^\top) \delta\left(f_{K,n'}^c - \frac{a_{n'}^c}{a_{n'}^1} [f_{K,n'}^1 - b_{n'}^1] - b_{n'}^c\right) df_{K,n}^1 df_{K,n'}^1 df_{K,n'}^c \\ &= \int_{f_{K,n}^1} \int_{f_{K,n'}^1} \left[\frac{a_{n'}^c}{a_{n'}^1} f_{K,n}^1 f_{K,n'}^1 - \frac{a_{n'}^c}{a_{n'}^1} b_{n'}^1 f_{K,n}^1 + b_{n'}^c f_{K,n}^1 \right] \mathcal{N}(\mathbf{f}_K^1 | \mathbf{b}^1, \mathbf{A}_1 K_\nu(\mathbf{X}, \mathbf{X}) \mathbf{A}_1^\top) df_{K,n}^1 df_{K,n'}^1 \\ &= \frac{a_{n'}^c}{a_{n'}^1} \left[a_{n'}^1 K_\nu(\mathbf{x}^n, \mathbf{x}^{n'}) a_{n'}^1 + b_{n'}^1 b_{n'}^1 \right] - \frac{a_{n'}^c}{a_{n'}^1} b_{n'}^1 b_{n'}^1 + b_{n'}^c b_{n'}^1 \\ &= a_{n'}^c a_{n'}^1 K_\nu(\mathbf{x}^n, \mathbf{x}^{n'}) + b_{n'}^c b_{n'}^1 \end{aligned} \quad (64)$$

yielding,

$$\begin{aligned}
\text{COV}[f_{K,n}^1, f_{K,n'}^c] &= \mathbb{E} [f_{K,n}^1 f_{K,n'}^c] - \mathbb{E} [f_{K,n}^1] \mathbb{E} [f_{K,n'}^c] \\
&= a_{n'}^c a_n^1 K_\nu(\mathbf{x}^n, \mathbf{x}^{n'}) + b_{n'}^c b_n^1 - b_n^1 b_{n'}^c \\
&= a_{n'}^c a_n^1 K_\nu(\mathbf{x}^n, \mathbf{x}^{n'})
\end{aligned} \tag{65}$$

Note that from the above integral is easy to see that $\text{COV}[f_{K,n'}^1, f_{K,n}^c] = a_n^c a_{n'}^1 K_\nu(\mathbf{x}^{n'}, \mathbf{x}^n)$.

A.3.3 Covariance between \mathbf{f}_K^1 and \mathbf{f}_K^c

We have derived the covariance between the *pivot* and any other process at the same location \mathbf{x}^n and between two different locations $\mathbf{x}^n, \mathbf{x}^{n'}$. Note that for N arbitrary locations \mathbf{X} , the covariance between any pair of elements can be obtained by any of the two derivations shown above.

In summary, at a given location \mathbf{x}^n the covariance between two processes is $a^c(\mathbf{x}^n) a^1(\mathbf{x}^n) K_\nu(\mathbf{x}^n, \mathbf{x}^n)$ and at two different locations \mathbf{x}^n and $\mathbf{x}^{n'}$ the covariance between two processes is $a^c(\mathbf{x}^{n'}) a^1(\mathbf{x}^n) K_\nu(\mathbf{x}^n, \mathbf{x}^{n'})$.

Thus, the covariance abetween the processes at N locations \mathbf{X} is given by $\mathbf{a}^1 (\mathbf{a}^c)^\top \odot K_\nu(\mathbf{X}, \mathbf{X})$.

A.4 Alternative derivation of Eq. 57

We found a simpler way of obtaining Eq. 57 by approximating the Dirac measure with a Gaussian and taking the limit of the variance to 0. With this, we can apply standard Gaussian integration and yield the desired result.

First:

$$\delta(\mathbf{f}_K^c - \mathbf{Q}\mathbf{f}_K^1 - \mathbf{r}) = \lim_{\lambda \rightarrow 0} \mathcal{N}(\mathbf{f}_K^c | \mathbf{Q}\mathbf{f}_K^1 + \mathbf{r}, \lambda \mathbf{I}) \tag{66}$$

and so the integral is solved by:

$$\begin{aligned}
p(\mathbf{f}_K^c) &= \lim_{\lambda \rightarrow 0} \int_{\mathbf{f}_K^1} \mathcal{N}(\mathbf{f}_K^1 | \mathbf{m}, \mathbf{S}) \mathcal{N}(\mathbf{f}_K^c | \mathbf{Q}\mathbf{f}_K^1 + \mathbf{r}, \lambda \mathbf{I}) d\mathbf{f}_K^1 \\
&= \lim_{\lambda \rightarrow 0} \mathcal{N}(\mathbf{f}_K^c | \mathbf{Q}\mathbf{m} + \mathbf{r}, \lambda \mathbf{I} + \mathbf{Q}\mathbf{S}\mathbf{Q}^\top) \\
&= \mathcal{N}(\mathbf{f}_K^c | \mathbf{Q}\mathbf{m} + \mathbf{r}, \mathbf{Q}\mathbf{S}\mathbf{Q}^\top)
\end{aligned} \tag{67}$$

A.5 Algebra manipulation of the Gaussian distribution

We are interested in showing:

$$\mathcal{N}(\mathbf{Q}^{-1}(\mathbf{f}_K - \mathbf{r}) | \mathbf{m}, \mathbf{S}) = \det \mathbf{Q} \mathcal{N}(\mathbf{f}_K | \mathbf{Q}\mathbf{m} + \mathbf{r}, \mathbf{Q}\mathbf{S}\mathbf{Q}^\top) \tag{68}$$

We provide the steps to be performed since we haven't found the steps available in the references searched. We can show this equivalence either by the technique of completing the square or by making simple manipulations to the exponent in the Gaussian distribution. We assume these Gaussian distributions have dimensionality n . Our manipulations use standard matrix operations that can be found in the matrix cookbook [31].

A.5.1 Manipulation of the exponent

We have:

$$\begin{aligned}
& \mathcal{N}(\mathbf{Q}^{-1}(\mathbf{f}_K - \mathbf{r}) \mid \mathbf{m}, \mathbf{S}) \\
&= \frac{1}{(2\pi)^{n/2}(\det \mathbf{S})^{1/2}} \exp \{ (\mathbf{Q}^{-1}(\mathbf{f}_K - \mathbf{r}) - \mathbf{m})^T \mathbf{S}^{-1} (\mathbf{Q}^{-1}(\mathbf{f}_K - \mathbf{r}) - \mathbf{m}) \} \\
&= \frac{1}{(2\pi)^{n/2}(\det \mathbf{S})^{1/2}} \exp \{ ((\mathbf{Q}^{-1}\mathbf{f}_K)^T - (\mathbf{Q}^{-1}\mathbf{r})^T - \mathbf{m}^T) \mathbf{Q}^T (\mathbf{Q}^T)^{-1} \mathbf{S}^{-1} \mathbf{Q}^{-1} \mathbf{Q} (\mathbf{Q}^{-1}\mathbf{f}_K - \mathbf{Q}^{-1}\mathbf{r} - \mathbf{m}) \} \\
&= \frac{1}{(2\pi)^{n/2}(\det \mathbf{S})^{1/2}} \exp \{ ((\mathbf{Q}^{-1}\mathbf{f}_K)^T \mathbf{Q}^T - (\mathbf{Q}^{-1}\mathbf{r})^T \mathbf{Q}^T - \mathbf{m}^T \mathbf{Q}^T) (\mathbf{Q}^{-1})^T \mathbf{S}^{-1} \mathbf{Q}^{-1} (\mathbf{f}_K - \mathbf{r} - \mathbf{Q}\mathbf{m}) \} \\
&= \frac{1}{(2\pi)^{n/2}(\det \mathbf{S})^{1/2}} \exp \{ (\mathbf{f}_K^T (\mathbf{Q}^T)^{-1} \mathbf{Q}^T - \mathbf{r}^T (\mathbf{Q}^T)^{-1} \mathbf{Q}^T - (\mathbf{Q}\mathbf{m})^T) (\mathbf{Q}^{-1})^T \mathbf{S}^{-1} \mathbf{Q}^{-1} (\mathbf{f}_K - \mathbf{r} - \mathbf{Q}\mathbf{m}) \} \\
&= \frac{1}{(2\pi)^{n/2}(\det \mathbf{S})^{1/2}} \exp \{ (\mathbf{f}_K^T - \mathbf{r}^T - (\mathbf{Q}\mathbf{m})^T) (\mathbf{Q}\mathbf{S}\mathbf{Q}^T)^{-1} (\mathbf{f}_K - \mathbf{r} - \mathbf{Q}\mathbf{m}) \} \\
&= \frac{1}{(2\pi)^{n/2}(\det \mathbf{S})^{1/2}} \exp \{ (\mathbf{f}_K - \mathbf{r} - \mathbf{Q}\mathbf{m})^T (\mathbf{Q}\mathbf{S}\mathbf{Q}^T)^{-1} (\mathbf{f}_K - \mathbf{r} - \mathbf{Q}\mathbf{m}) \}
\end{aligned} \tag{69}$$

This gives an unnormalized Gaussian distribution with mean $\mathbf{Q}\mathbf{m} + \mathbf{r}$ and covariance $\mathbf{Q}\mathbf{S}\mathbf{Q}^T$

A.5.2 Completing the square method

We can obtain a similar result by the technique of completing the square. Since we know that a scale and shift on a function argument does not change the function shape, i.e. scaling and shifting a Gaussian will give a Gaussian curve, we can use the technique of completing the square to recognize the mean and covariance matrix [5].

From:

$$\begin{aligned}
& \mathcal{N}(\mathbf{Q}^{-1}(\mathbf{f}_K - \mathbf{r}) \mid \mathbf{m}, \mathbf{S}) \\
&= \frac{1}{(2\pi)^{n/2}(\det \mathbf{S})^{1/2}} \exp \{ (\mathbf{Q}^{-1}(\mathbf{f}_K - \mathbf{r}) - \mathbf{m})^T \mathbf{S}^{-1} (\mathbf{Q}^{-1}(\mathbf{f}_K - \mathbf{r}) - \mathbf{m}) \}
\end{aligned} \tag{70}$$

We expand the quadratic form:

$$\begin{aligned}
& (\mathbf{Q}^{-1}(\mathbf{f}_K - \mathbf{r}) - \mathbf{m})^T \mathbf{S}^{-1} (\mathbf{Q}^{-1}(\mathbf{f}_K - \mathbf{r}) - \mathbf{m}) \\
&= (\mathbf{Q}^{-1}(\mathbf{f}_K - \mathbf{r}))^T \mathbf{S}^{-1} (\mathbf{Q}^{-1}(\mathbf{f}_K - \mathbf{r})) - 2(\mathbf{Q}^{-1}(\mathbf{f}_K - \mathbf{r}))^T \mathbf{S}^{-1} \mathbf{m} + \mathbf{m}^T \mathbf{S}^{-1} \mathbf{m} \\
&= (\mathbf{Q}^{-1}\mathbf{f}_K)^T \mathbf{S}^{-1} \mathbf{Q}^{-1}\mathbf{f}_K - (\mathbf{Q}^{-1}\mathbf{f}_K)^T \mathbf{S}^{-1} \mathbf{Q}^{-1}\mathbf{r} - (\mathbf{Q}^{-1}\mathbf{r})^T \mathbf{S}^{-1} \mathbf{Q}^{-1}\mathbf{f}_K \\
&+ (\mathbf{Q}^{-1}\mathbf{r})^T \mathbf{S}^{-1} \mathbf{Q}^{-1}\mathbf{r} - 2(\mathbf{Q}^{-1}\mathbf{f}_K)^T \mathbf{S}^{-1} \mathbf{m} + 2(\mathbf{Q}^{-1}\mathbf{r})^T \mathbf{S}^{-1} \mathbf{m} + \mathbf{m}^T \mathbf{S}^{-1} \mathbf{m}
\end{aligned} \tag{71}$$

and first recognize the terms depending quadratically on \mathbf{f}_K :

$$\begin{aligned}
& (\mathbf{Q}^{-1}\mathbf{f}_K)^T \mathbf{S}^{-1} \mathbf{Q}^{-1}\mathbf{f}_K = \mathbf{f}_K^T (\mathbf{Q}^{-1})^T \mathbf{S}^{-1} \mathbf{Q}^{-1}\mathbf{f}_K \\
&= \mathbf{f}_K^T (\mathbf{Q}^T)^{-1} \mathbf{S}^{-1} \mathbf{Q}^{-1}\mathbf{f}_K \\
&= \mathbf{f}_K^T (\mathbf{Q}\mathbf{S}\mathbf{Q}^T)^{-1} \mathbf{f}_K
\end{aligned} \tag{72}$$

Recognizing the covariance to be $\mathbf{Q}\mathbf{S}\mathbf{Q}^T$. Now looking at the terms that depend linearly on \mathbf{f}_K we have:

$$\begin{aligned}
& -(\mathbf{Q}^{-1}\mathbf{f}_K)^T \mathbf{S}^{-1} \mathbf{Q}^{-1}\mathbf{r} - (\mathbf{Q}^{-1}\mathbf{r})^T \mathbf{S}^{-1} \mathbf{Q}^{-1}\mathbf{f}_K - 2(\mathbf{Q}^{-1}\mathbf{f}_K)^T \mathbf{S}^{-1} \mathbf{m} \\
&= -\mathbf{f}_K^T (\mathbf{Q}^{-1})^T \mathbf{S}^{-1} \mathbf{Q}^{-1}\mathbf{r} - \mathbf{r}^T (\mathbf{Q}^{-1})^T \mathbf{S}^{-1} \mathbf{Q}^{-1}\mathbf{f}_K - 2\mathbf{f}_K^T (\mathbf{Q}^{-1})^T \mathbf{S}^{-1} \mathbf{m} \\
&= -\mathbf{f}_K^T (\mathbf{Q}\mathbf{S}\mathbf{Q}^T)^{-1} \mathbf{r} - \mathbf{r}^T (\mathbf{Q}\mathbf{S}\mathbf{Q}^T)^{-1} \mathbf{f}_K - 2\mathbf{f}_K^T (\mathbf{Q}^{-1})^T \mathbf{S}^{-1} \mathbf{m}
\end{aligned} \tag{73}$$

Looking closely at $\mathbf{r}^T (\mathbf{Q}\mathbf{S}\mathbf{Q}^T)^{-1} \mathbf{f}_K$ we have:

$$\begin{aligned}
& \mathbf{r}^T (\mathbf{Q}\mathbf{S}\mathbf{Q}^T)^{-1} \mathbf{f}_K = \mathbf{f}_K^T ((\mathbf{Q}\mathbf{S}\mathbf{Q}^T)^{-1})^T \mathbf{r} \\
&= \mathbf{f}_K^T ((\mathbf{Q}\mathbf{S}\mathbf{Q}^T)^T)^{-1} \mathbf{r} \\
&= \mathbf{f}_K^T (\mathbf{Q}\mathbf{S}^T \mathbf{Q}^T)^{-1} \mathbf{r} \\
&= \mathbf{f}_K^T (\mathbf{Q}\mathbf{S}\mathbf{Q}^T)^{-1} \mathbf{r}
\end{aligned} \tag{74}$$

since \mathbf{S} is symmetric i.e. $\mathbf{S} = \mathbf{S}^T$. This yields a final linear term given by:

$$-\mathbf{f}_K^T(\mathbf{Q}\mathbf{S}\mathbf{Q}^T)^{-1}\mathbf{r} - \mathbf{f}_K^T(\mathbf{Q}\mathbf{S}\mathbf{Q}^T)^{-1}\mathbf{r} - 2\mathbf{f}_K^T(\mathbf{Q}^{-1})^T\mathbf{S}^{-1}\mathbf{m} \quad (75)$$

By rewriting $-2\mathbf{f}_K^T(\mathbf{Q}^{-1})^T\mathbf{S}^{-1}\mathbf{m}$ as:

$$\begin{aligned} -2\mathbf{f}_K^T(\mathbf{Q}^{-1})^T\mathbf{S}^{-1}\mathbf{m} &= -2\mathbf{f}_K^T(\mathbf{Q}^{-1})^T\mathbf{S}^{-1}\mathbf{Q}^{-1}\mathbf{Q}\mathbf{m} \\ &= -2\mathbf{f}_K^T(\mathbf{Q}\mathbf{S}\mathbf{Q}^T)^{-1}\mathbf{Q}\mathbf{m} \end{aligned} \quad (76)$$

We obtain the final desired linear term:

$$\begin{aligned} &-\mathbf{f}_K^T(\mathbf{Q}\mathbf{S}\mathbf{Q}^T)^{-1}\mathbf{r} - \mathbf{f}_K^T(\mathbf{Q}\mathbf{S}\mathbf{Q}^T)^{-1}\mathbf{r} - 2\mathbf{f}_K^T(\mathbf{Q}^{-1})^T\mathbf{S}^{-1}\mathbf{m} = \\ &-2\mathbf{f}_K^T(\mathbf{Q}\mathbf{S}\mathbf{Q}^T)^{-1}\mathbf{r} - 2\mathbf{f}_K^T(\mathbf{Q}\mathbf{S}\mathbf{Q}^T)^{-1}\mathbf{Q}\mathbf{m} \\ &= -2\mathbf{f}_K^T(\mathbf{Q}\mathbf{S}\mathbf{Q}^T)^{-1}[\mathbf{Q}\mathbf{m} + \mathbf{r}] \end{aligned} \quad (77)$$

Recognizing $\mathbf{Q}\mathbf{m} + \mathbf{r}$ as the mean of the distribution.

Finally, we would have to check if there is a way for the remaining constant terms to be re-written as $[\mathbf{Q}\mathbf{m} + \mathbf{r}]^T\mathbf{S}^{-1}[\mathbf{Q}\mathbf{m} + \mathbf{r}]$ otherwise the probability density would not be correctly normalized. Since we know from the previous section that this yields an unnormalized density we omit this step. Anyway we can skip this step since we know that function argument scaling is a non-volume preserving transformation, something that can be trivially checked by computing the area of a function $x(t) = u(t) - u(t-1)$ and its scaled version $x(2t)$, where $u(t)$ is the unit (or Heaviside) step function.

This can be more formally check if we consider the probability under change of variable. If we have $\mathbf{y} = f(\mathbf{x})$ for some invertible function $f(\cdot)$ with $\mathbf{y} \sim p(\mathbf{y})$, then:

$$p(\mathbf{x}) = p(\mathbf{y} = f(\mathbf{x})) \left| \det \frac{\nabla f(\mathbf{x})}{\mathbf{x}} \right| \quad (78)$$

for a linear transformation $\mathbf{y} = \mathbf{Q}\mathbf{x} + \mathbf{r}$, this gives:

$$p(\mathbf{x}) = p(\mathbf{y} = \mathbf{Q}\mathbf{x} + \mathbf{r}) |\det \mathbf{Q}| \quad (79)$$

formally showing that a scale in the argument of a density implies a non-volume preserving transformation and thus without the Jacobian correction it would not be a proper normalized density.

A.5.3 The remaining normalization constant

It is clear that the scaling of the Gaussian argument gives an unnormalized density with mean $\mathbf{Q}\mathbf{m} + \mathbf{r}$ and covariance $\mathbf{Q}\mathbf{S}\mathbf{Q}^T$. A proper normalized Gaussian density would have a multiplication constant equal to:

$$\frac{1}{(2\pi)^{n/2}(\det \mathbf{Q}\mathbf{S}\mathbf{Q}^T)^{1/2}} \quad (80)$$

but our result has:

$$\frac{1}{(2\pi)^{n/2}(\det \mathbf{S})^{1/2}} \quad (81)$$

Operating the determinant we see:

$$\begin{aligned} (\det \mathbf{Q}\mathbf{S}\mathbf{Q}^T)^{1/2} &= (\det \mathbf{Q} \det \mathbf{S} \det \mathbf{Q}^T)^{1/2} \\ &= (\det \mathbf{S})^{1/2}(\det \mathbf{Q} \det \mathbf{Q})^{1/2} = (\det \mathbf{S})^{1/2} |\det \mathbf{Q}| \end{aligned} \quad (82)$$

where since the determinant is a scalar value we know that $\sqrt{x^2} = |x|$. This means that we need to scale our density by $1/|\det \mathbf{Q}|$, or, in other words, our density has been unnormalized by multiplying it by $|\det \mathbf{Q}|$. With this, we conclude:

$$\mathcal{N}(\mathbf{Q}^{-1}(\mathbf{f}_K - \mathbf{r}) \mid \mathbf{m}, \mathbf{S}) = |\det \mathbf{Q}| \mathcal{N}(\mathbf{f}_K \mid \mathbf{Q}\mathbf{m} + \mathbf{r}, \mathbf{Q}\mathbf{S}\mathbf{Q}^T) \quad (83)$$

B Experiment Appendix

In this appendix we provide training/evaluation details alongside additional results.

Information about the different datasets used can be found in the code, where a link to the website of each particular dataset can be found. Information about dataset preprocessing can also be found in the code since datasets are very different (images, tabular, tabular with discrete inputs etc) and so different preprocessing was done. General preprocessing steps are the normalization to $[0, 1]$ range of image datasets, normalization by the mean and standard deviation in continuous tabular datasets, and different normalization procedures depending on the type of feature. For example, a dataset containing working age information was normalized by dividing by 65 since that is the maximum number of years (on average) of a standard worker’s life.

Common to all experiments is the following information. Experiments are run using GPFLOW [29, 45]. Unless mentioned we use default GPFLOW parameters. Inducing points are initialized using Kmeans algorithm for `vowel,absenteeism` and `avila` with 10 reinitializations and parallel Kmeans for `characterfont` and `devangari` with 3 reinitializations. The length scale of RBF kernels was initialized to 2.0 and the mixing matrix randomly. Non-stationary kernels are initialized with a length scale of 2.0 for the arcosine and with an identity matrix for the Neural Network kernel. All kernels employ automatic relevance determination if possible. The variational mean is initialized to zero and the Cholesky factorization of the variational covariance to the identity matrix multiplied by $1e - 5$. In all the experiments the model used to compute the train/valid/test metrics was the model corresponding to the epoch with best (highest) ELBO. We use Adam optimizer.

For all the SVGP models we run models with learning rate values of 0.01 and 0.001. For certain choices of hyper-parameters if we saw that 0.01 was providing better results than 0.001 we keep searching just with 0.01. In some cases we also look for other learning rates e.g. 0.05 in light of finding the best baseline model to compare against. We run either 10000 or 15000 epochs for `vowel,absenteeism` and `avila` and 100, 200, 500, 1000, 2000 epochs for `characterfont` and `devangari`. For these last two dataset we do not always launch 2000 epochs, and only did it if we found a big increase in performance from the run with 500 to 1000 epochs. Note that training times are average over epochs and we do not provide the full time of the experiment (which in turns imply that the ETGP is even faster since we run them just for 500 epochs). We run models with number of inducing points $\{100, 50, 20\}$ for (`vowel,absenteeism` and `avila`) and 100 for `characterfont` and `devangari`. We also experiment with the parameters of the covariance (including the mixing matrix parameters in RBFCORR) being freezed for 2000 (`vowel,absenteeism` and `avila`) or 50 (`characterfont` and `devangari`) epochs or trained end to end, i.e. no freezing is applied, following [28, 20]. Once all these experiments were launched, we select for each set of kernel, number of inducing points etc, the model giving the best performance by directly looking at the test set, in order to evaluate the proposed model in the most optimistic situation for each SVGP baseline.

For the ETGP model selection was done using a validation split with different number of points per dataset. This information is provided by looking at the code that loads the data. For the ETGP all the models are run for 15000 epochs for `vowel,absenteeism` and `avila` and 500 epochs for `characterfont` and `devangari` (which implies that the total training time of our models is even faster), and the best selected model on validation for 100 inducing points, is run for 50 and 20, in contrast with SVGP where each 50 and 20 inducing points model can have its own set of training hyperparameters. Bayesian flows are trained with 1 Monte Carlo dropout sample and evaluated (i.e. posterior predictive computation) using 20 dropout samples. The learning rate experimented was 0.01 and 0.001 and all the parameters are trained from the beginning without freezing. The NN architectures were chosen depending on the input size of the dataset. All these architectures have an input layer equal to the dimensionality of the data and an output layer given by the number of parameters of the flow multiplied by the number of classes. We tested LINEAR, SAL [34] with length 3 and TANH [38] with length 3 and 4 elements in the linear combination. The length of the flow corresponds to the value of K in the flow parameterization, i.e. it is the number of, e.g. individual SAL transformations, being concatenated. All the NN use hyperbolic tangent activation function and we use a variance of a Gaussian prior over flow parameters set to 5000, 50000, 50000 which corresponds to a weight decay factor of $1e - 4, 1e - 5, 1e - 6$ without considering the constant value of the Gaussian prior that depends on the number of parameters. For `vowel,absenteeism` and `avila` we test networks with 0, 1, 2 hidden layers with 25, 50, 100 neurons per layer and with dropout probabilities of 0.25, 0.5, 0.75 except `avila` that only uses 0.25, 0.5. We tested 0.75 to see if higher

uncertainty in the NN posterior could help in regularizing the datasets with fewer number of training points. For `devangari` we test 0, 1, 2 hidden layers with 512, 1024 neurons per layer. We also tested a projection network of 0, 1 hidden layers with 512 neurons per hidden layer and 256 neurons per output layer. The output of this projection network is feed into another neural network that maps the 256 dimensions to the number of parameters. This second NN has 0, 1 hidden layers with 256, 128 neurons per layer. All these networks have a dropout probability of 0.5. For `characterfont` we also use a dropout probability of 0.5 and NN with 0, 1, 2 hidden layers with 256 neuron per layer. We also test projection networks of 0, 1, 2 hidden layers with 512, 256 neuron per hidden layer and output layer of 256 neurons. This is then feed into another neural network with 0, 1, 2 hidden layers and 256 neuron per layer.

Regarding the initialization of the flows we follow [28] and initialize the flows to the identity by first learning the identity mapping using a non-input dependent flow, and then learning the parameters of the neural network to match each point in the training dataset to the learned non-input dependent parameters. Both initialization procedures are launched 5 times with a learning rate of 0.05 and Adam optimizer for any dataset and flow architecture. The input dependent initialization is run for 1000 epochs in `vowel,absenteeism` and `avila` and for 100 epochs in `characterfont` and `devangari`. Some preliminary runs were done to test if these hyperparameters allow the flow to be properly initialized and then all these parameters were used for any flow initialization in our validation search without further analysis. We found in general that with fewer epochs the flow could be also initialized properly, but decided to run a considerable number of initialization epochs. We highlight that this procedure can be done in parallel to Kmeans initialization, for readers concerned with the training time associated with this initialization procedure.

B.1 Log Likelihood results

In this subsection we provide the corresponding LL results in Fig. 7 and Fig. 8 which are discussed in the main text.

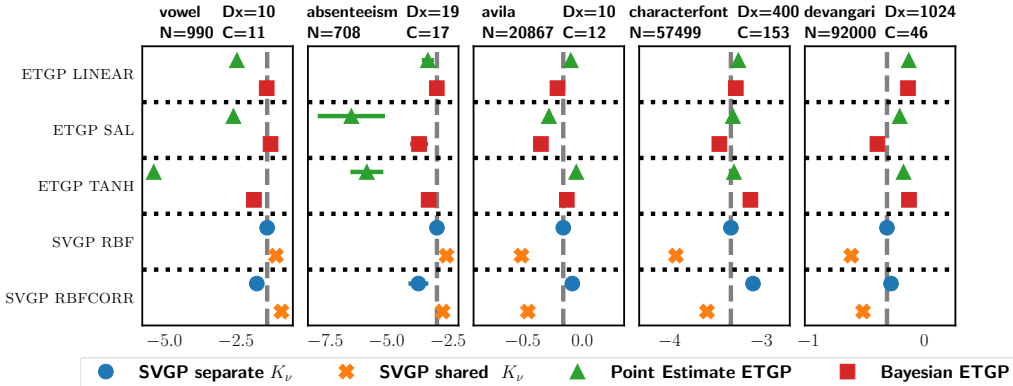


Figure 7: Log Likelihood (right is better) comparing the proposed model against independent/dependent stationary GPs.

B.2 SAL flow discussion

In the work from [28] input dependent TGPs only used the SAL flow parameterization. These flows have the good property that they can recover the identity function, see [34], making them suitable for these applications since the marginal likelihood can penalize complexity in the warping function and ‘choose’ to use a GP by setting a linear mapping.

In this work, we have shown that SAL flows provide, in general, worse results than the TANH or LINEAR flows. On one side, this shows the potential improvements that can be achieved by the versatility of the different flows that can be parameterized. Beyond being able to control moments of the induced distributions [34], different flows combination can be more expressive or more training stable.

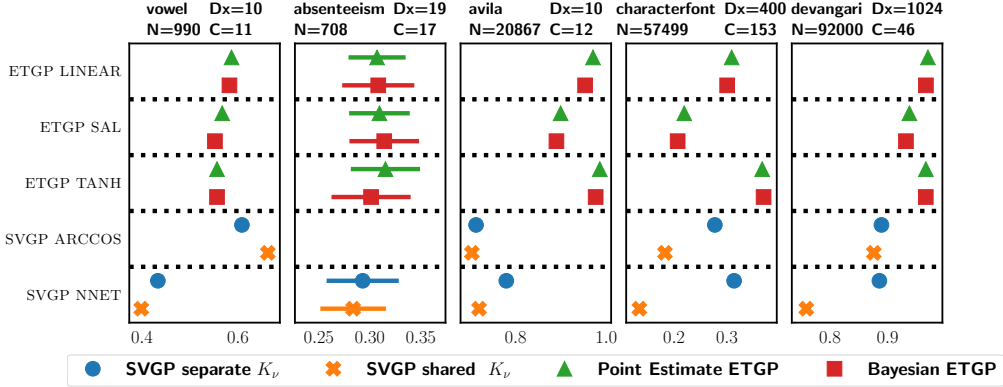


Figure 8: Log Likelihood (right is better) comparing the proposed model against non-stationary GPs.

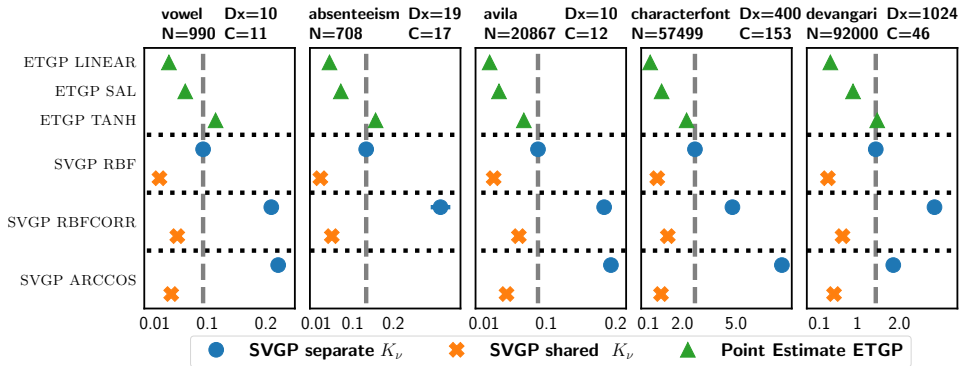


Figure 9: Average training time per epoch in minutes (left is better) comparing ETGP with SVGPs. NNET kernel is omitted as it is slower.

In particular, a problem with the SAL flow is that small changes in its parameters can lead to mappings with a high derivative (like an exponential curve). This implies a big change in the gradients and thus while training we can suffer either from numerical saturation or convergence issues. This can be a possible explanation for this performance drop. In fact, in our experiments, we found SAL to be the most saturating flow.

Nevertheless, exploring architectures with fewer parameters, such as SAL flows, that can learn arbitrary non linear mappings such as those of TANH, are an interesting line of research. For example the TANH flow used has 12 parameter, which implies an output NN layer of 1836 neurons for $C = 153$ which considerably increases the computational burden when making Bayesian predictions, and also affects the speed improvement obtained. Anyway, this flow has similar training runs as SVGP while providing much better metrics.

B.3 Prediction time results

We provide the average prediction time results in Fig. 9, where we can see a similar trend as in the training time results. Our model can be one order of magnitude faster while providing similar or better prediction results. We can see how the reimplemention discussed in App. C boost the computational performance of the SVGP RBFCORR considerably.

B.4 Using less inducing points

In the final part of the appendix we provide additional results with less inducing points. We provide results with 50, 20 inducing points and the LL in Fig. 10 and Fig. 11.

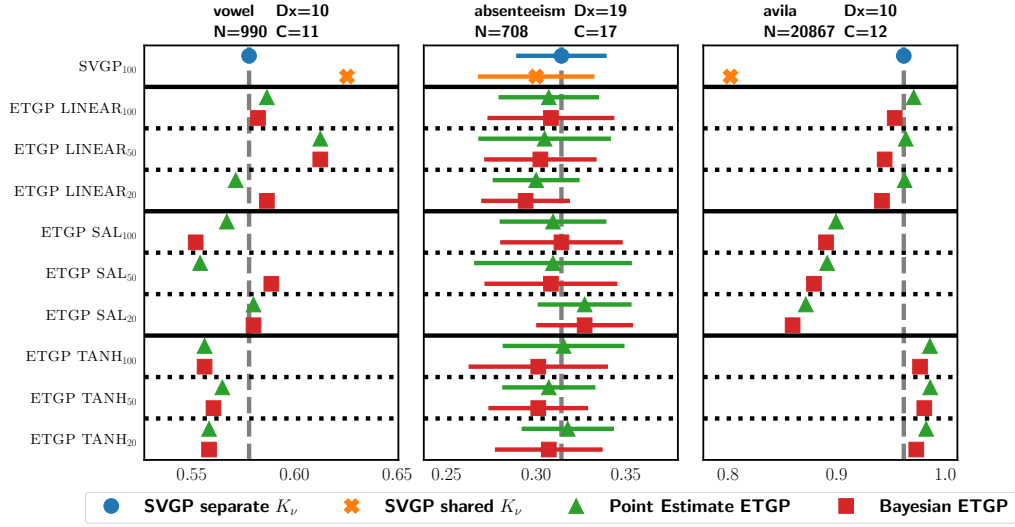


Figure 10: Results comparing ACC (right is better) using less inducing points.

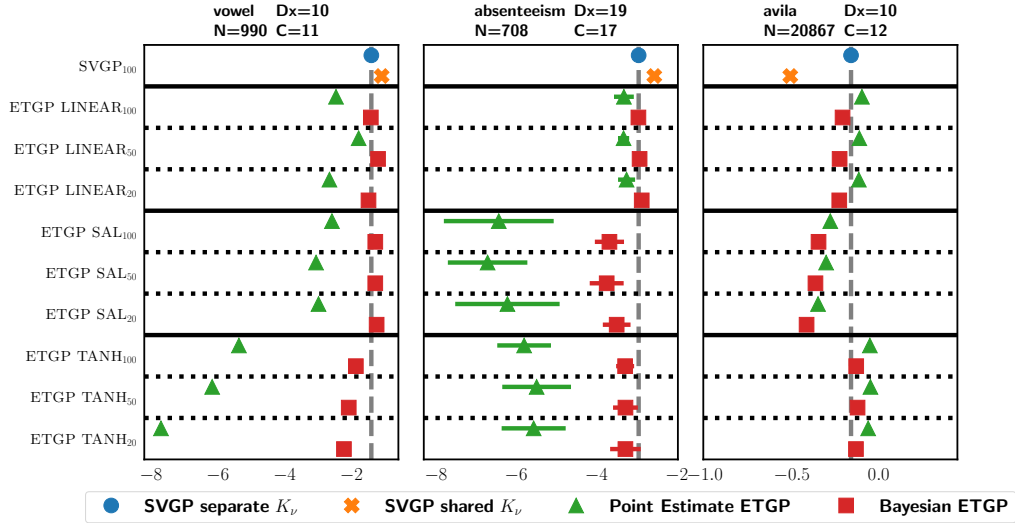


Figure 11: Results comparing LL (right is better) using less inducing points.

We observe how using less inducing points can regularize or provide an improvement over the SVGP. We also see how the Bayesian flow provides, in the fewer inducing points setting, better results than the point estimate. This is specially significant in terms of LL.

C Refactorizing GPFLOW source code

In our experiments we found an issue in the source code of GPFLOW, which considerably speed-up the performance of SVGPs where the kernel is shared. We used GPFLOW version 2.1.3 and have found that the current issue also appears in the last stable version 2.5.2. However, since the source code has considerably changed, our provided implementation is only valid for the earlier version.

We refactorize the source code in a way that is clear where the issue comes from, but note that better refactorizations could be done but would require a high-level and careful check of all the elements involved and how it would generalize to other computations.

The computation is concerned with the evaluation of the marginal variational distribution:

$$q(f_0^c) = \mathcal{N}(f_{0,n}^c | K_{\nu^c \mathbf{x}, \mathbf{z}^c}^c K_{\nu^c \mathbf{z}^c, \mathbf{z}^c}^c{}^{-1} \mathbf{m}^c, K_{\nu^c \mathbf{x}, \mathbf{x}}^c - K_{\nu^c \mathbf{z}^c, \mathbf{z}^c}^c{}^{-1} [K_{\nu^c \mathbf{z}^c, \mathbf{z}^c}^c + \mathbf{S}^c] K_{\nu^c \mathbf{z}^c, \mathbf{z}^c}^c{}^{-1} K_{\nu^c \mathbf{z}^c, \mathbf{x}}^c)$$

of each of the C latent processes when they are later mixed by a mixing matrix. If we see, for a batch of samples \mathbf{X} we need to evaluate $K_{\nu^c \mathbf{x}, \mathbf{x}}^c$ C times if the kernel is not shared and only 1 if the kernel is shared. We found GPFLOW to always evaluate it C times regardless of the type of kernel when a mixing matrix is later applied. In GPFLOW version 2.1.3 we can see that the LinearCoregionalization kernel does not differentiate if the latent GP is shared or not, see <https://github.com/GPflow/GPflow/blob/v2.1.3/gpflow/kernels/multioutput/kernels.py> line 174. Thus, when computing the covariance, we can see in line 130 here <https://github.com/GPflow/GPflow/blob/v2.1.3/gpflow/conditionals/multioutput/conditionals.py> that the evaluation is performed C times when it would be easier to evaluate it just once, and then tile C times, which is the basic refactorization we perform. Also note that if the inducing points are not shared, but the kernel is, GPFLOW would also perform this inefficient computation (see line 129 where the kernel instance is repeated C times). When the inducing points are shared and an independent kernel (no mixing matrix) is used, then GPFLOW runs computations correctly (see lines 46 and 92).

We observed similar issues in the newest GPFLOW version 2.5.2. We see that the LinearCoregionalization kernel in <https://github.com/GPflow/GPflow/blob/v2.5.2/gpflow/kernels/multioutput/kernels.py> line 199 do not make distinctions on whether the latent kernel is shared or not and this kernel is still inheriting from "Combination" class. Thus, the dispatcher in <https://github.com/GPflow/GPflow/blob/v2.5.2/gpflow/posteriors.py> will not perform the computation starting in 778 (note it checks if the kernel is SharedIndependent but LinearCoregionalization is type Combination) but that starting in 791, which again evaluates the kernel C times.

We found several improvements that can be done to GPFLOW source code and we will open corresponding issues and list them under our Github implementation of this work. We think that this particular one could be easily solved by using a LMC kernel for latent shared kernel and a LMC for latent separate independent kernel; or by explicitly checking if the elements in the underlying kernel list share references; or by, easily, using a list with just one element if the kernel is shared and C elements if the kernel is not shared; or by wrapping around SharedIndependent or SeparateIndependent kernels base classes instead of using a list containing the kernels.

Another option, as employed by GPYTORCH [17], could be to evaluate the kernel directly using batched computations. We believe that the computational bottleneck comes from performing the kernel evaluation using a loop in python. This is because computing the squared distance in most kernels has a linear cost, so at most the corresponding added complexity should be $\mathcal{O}(Cd)$, with d the dimensionality of the data. However, we found that without doing our improvement the code was much slower. Thus we further believe that computing the squared distance using batched computations rather than loops would also bridge the gap between the computational times of the SVGP with a separate kernel and the ETGP. Nevertheless our model is still competitive or even provides better results and faster since cubic computations do not scale linearly with C which in a quick code snippet in TENSORFLOW we found to be 1 order of magnitude slower for $C = 153$ and $M = 100$ and 5 times slower for $C = 10$. The code snippet is:

```
1 import tensorflow as tf
2 import time
3 import numpy as np
4
5 C = 10
6 runs = 100
7
8
9 X_ = np.random.randn(1,100,100)
10 X = X_@X_.transpose(0,2,1)
11 X = tf.constant(X)
12
13 Y_ = np.random.randn(C,100,100)
14 Y = Y_@Y_.transpose(0,2,1)
15 Y = tf.constant(Y)
16
17 acc = 0.0
18 for i in range(runs):
19     start = time.process_time();
20     tf.linalg.cholesky(X);
21     acc += time.process_time()-start
22 print(acc/runs)
23
24 acc = 0.0
25 for i in range(runs):
26     start = time.process_time();
27     tf.linalg.cholesky(Y);
28     acc += time.process_time()-start
29 print(acc/runs)
```
